Московский институт электронной техники (МИЭТ)

На правах рукописи

УДК 519.6

Mikhail Evgenievich Lebedev

Stationary Solutions of Gross–Pitaevskii Equation with Periodically Modulated Nonlinearity

05.13.18 – Математическое моделирование, численные методы и комплексы программ

ДИССЕРТАЦИЯ

на соискание ученой степени

кандидата физико-математических наук

Научный руководитель

д. ф.-м. н., проф.

G. L. Alfimov

Moscow – 2021

Contents

Itroduction

One dimensional Gross–Pitaevskii equation (describes "cigar-shaped" condensate) takes form:

$$i\Psi_t + \Psi_{xx} + U(x)\Psi + P(x)|\Psi|^2\Psi = 0. \qquad (1)$$

Here $\Psi(t,x)$ is the macroscopic wave function of the condensate, $U(x)$ corresponds to the potential of the trap holding the condensate, and $P(x)$ describes characteristic length of the atomic interactions. Function $P(x)$ is called as *pseudopotential* which is induced by spatial periodic modulation. This can be achieved in BEC by means of the Feshbach resonance controlled by magnetic or optical field [1–3]. In the nonlinear optics spatial modulation of the Kerr coefficient can be induced by inhomogeneous density of resonant nonlinearity-enhancing dopants implanted into the waveguide [4].

...

Chapter 1

General Propositions on Regular and Singular Solutions for Stationary States Equation $u_{xx} + Q(x)u + P(x)u^3 = 0$

1.1. Objections

In this chapter our main goal is to formulate general propositions about singular and regular solutions for the general form of the stationary states equation.

$$u_{xx} + Q(x)u + P(x)u^3 = 0. \tag{1.1}$$

As it was shown previously this equation follows from the original Gross–Pitaevskii equation by the the substitution

$$\Psi(t, x) = u(x)e^{-i\omega t}, \tag{1.2}$$

where the corresponding localization conditions allow us to consider $u(x)$ as a real-valued function.

We suppose that functions $Q(x), P(x) \in C^1(\mathbb{R})$ and will put additional restrictions further when it's needed. Mainly we are interested in two main cases: (A) when do exist regular solutions; and (B) what are the conditions on function $Q(x)$ and $P(x)$ which can guarantee the existence of the singular solutions for the equation (2.1), and what is the behaviour of the collapsing solutions near the collapse point. In this chapter partial answer to question (A) is given by the Propositions 1 and 2. On the other hand Proposition 3 gives a partial answer to the question (B). It states that if the function $P(x)$ less then zero at least at one point $x = x_0$ then there exist two one-parametric families of solutions collapsing at x_0.

1.2. Absence of the Singular Solutions: $P(x) \geq P_0 > 0$

This section contains a sufficient condition for absence of singular solutions of the equation (2.1). It's given by the following proposition.

Proposition 1. *Let $\forall x$ functions $Q(x), P(x) \in C^1(\mathbb{R})$, moreover:*

(a) $P(x) \geq P_0 > 0$, $|P'(x)| \leq \widetilde{P}$;

(b) $Q(x) \geq Q_0$, $|Q'(x)| \leq \widetilde{Q}$;

then solution of the Cauchy problem for the equation (2.1) *with arbitrary initial conditions* $u(x_0) = u_0$, $u_x(x_0) = u_0'$ *can be continued to the whole real axis* $\mathbb{R}$.

Proof. By the existence and uniqueness theorem for ODE there exists an interval $[x_0; x_1)$ such that a solution of the Cauchy problem $u(x)$ for the equation (2.1) with initial conditions $u(x_0) = u_0$, $u_x(x_0) = u_0'$ exists and is unique on the interval, $u(x) \in C^2[x_0; x_1)$. Suppose that $[x_0; x_1)$ is the maximum interval of existence for the the solution $u(x)$. It means that solution of the Cauchy problem $u(x)$ cannot be continued beyond the point x_1. Multiply the original equation by $4u_x(x)$ and then integrate it over $[x_0, x)$, $x < x_1$, we have the following relationship:

$$2u_x^2(x)) + 2Q(x)u^2(x) - 2\int\limits_{x_0}^{x} Q'(\xi)u^2(\xi)d\xi + P(x)u^4(x) - \int\limits_{x_0}^{x} P'(\xi)u^4(\xi)d\xi =$$
$$= 2(u_0')^2 + 2Q(x_0)u_0^2 + P(x_0)u_0^4 \equiv C. \tag{1.3}$$

We can omit term $u_x^2(x) \geq 0$ in the left-hand side of the equality, and take into account the lower limits for $Q(x)$, $P(x)$ functions, so we come to the following inequality:

$$2Q_0u^2(x) + P_0u^4(x) \leq C + 2\int\limits_{x_0}^{x} Q'(\xi)u^2(\xi)d\xi + \int\limits_{x_0}^{x} P'(\xi)u^4(\xi)d\xi. \tag{1.4}$$

Further we can replace the derivatives $Q'(\xi)$ and $P'(\xi)$ with their upper bounds: $Q'(\xi) \leq \widetilde{Q}$, $P'(\xi) \leq \widetilde{P}$, where $\widetilde{Q} \geq 0$, $\widetilde{P} \geq 0$. With multiplying both sides of the inequality by P_0, we have

$$2Q_0P_0u^2(x) + P_0^2u^4(x) \le P_0C + 2P_0\widetilde{Q}\int\limits_{x_0}^{x} u^2(\xi)d\xi + P_0\widetilde{P}\int\limits_{x_0}^{x} u^4(\xi)d\xi. \tag{1.5}$$

Let $v(x) = (P_0u^2(x) + Q_0)^2$, $v(x) \ge 0$, substituting this into (1.5) gives

$$v(x) \le \widetilde{C} + \frac{\widetilde{P}}{P_0}\int\limits_{x_0}^{x} w(v(\xi))d\xi. \tag{1.6}$$

Here $\widetilde{C} = P_0C + Q_0^2 \ge 0$, $\alpha = 2\widetilde{Q}P_0/\widetilde{P} \ge 0$, and $w(v)$ is defined by

$$w(v) \equiv \alpha(\sqrt{v} - Q_0) + (\sqrt{v} - Q_0)^2. \tag{1.7}$$

Consider the following function

$$G(s) = \int\limits_{s_0}^{s} \frac{dv}{w(v)}. \tag{1.8}$$

Here $s_0 > Q_0^2$ is an arbitrary constant, $s \ge s_0$. Since $w(v)$ is a positive and monotonically decreasing function, and the integral

$$\int\limits_{s_0}^{+\infty} \frac{dv}{w(v)} \tag{1.9}$$

diverges, one can conclude that $G(s)$ is a positive, monotonically increasing, and unbounded function. It means that an inverse function $G^{-1}(r)$ is well-defined for $r \ge 0$, increases monotonically, and is unbounded. The above-mentioned statements allow as to apply *Bihary* inequality [5, theorem 2.3.1] to (1.6) which allows us to conclude that:

$$v(x) \le G^{-1}\left(G(\widetilde{C}) + \frac{\widetilde{P}}{P_0}\int\limits_{x_0}^{x} d\xi\right) = G^{-1}\left(G(\widetilde{C})\frac{\widetilde{P}}{P_0}(x - x_0)\right) < \infty. \tag{1.10}$$

Inequality (1.10) is valid for all $x \in [x_0; x_1)$. It follows from (1.10) that function $v(x)$ is bounded on the whole segment $[x_0; x_1)$:

$$v(x) \le M = G^{-1}\left(G(\widetilde{C}) + \frac{\widetilde{P}}{P_0}(x_1 - x_0)\right). \tag{1.11}$$

We observe that $\widetilde{C} \geq Q_0^2$, moreover $\widetilde{C} = Q_0^2$ only if $u_0 = u_0' = 0$. It means that $G(s)$ is well-defined for each constant $\widetilde{C}$ corresponding to any non-zero solution $u(x)$. The boundedness of $v(x)$ yields that solution $u(x)$ is also bounded on the segment $[x_0; x_1)$:

$$|u(x)| \leq \sqrt{\frac{\sqrt{M} - Q_0}{P_0}}, \quad x \in [x_0; x_1). \tag{1.12}$$

Substitution of the estimate (1.12) into the identity (1.3) gives the upper bound for the derivative $u_x(x)$ on the interval $x \in [x_0; x_1)$. Since functions $u(x)$ and $u_x(x)$ are continuous and bounded on $[x_0; x_1)$, the values $u(x_1) = u_1$ and $u_x(x_1) = u_1'$ are finite. Hence there exists a continuation of the solution to the Cauchy problem with the initial conditions $u(x_0) = u_0$, $u_x(x_0) = u_0'$ on a larger interval beyond the initial $[x_0; x_1)$. It contradicts to the original assumption.

Thus we have proven the possibility of continuation of the solution to the half-line $x > x_0$. In order to prove the same statement for $x < x_0$, one can make a substitution $x \to -x$ and repeat the above-mentioned proof. $\square$

One trivial corollary simply follows from this proposition.

Corollary 1. *If the conditions (a) and (b) are satisfied not on the whole real axis* $\mathbb{R}$*, but only on some segment* $[x_1; x_2]$*, then a solution of the Cauchy problem for the equation* (2.1) *with arbitrary initial conditions does not collapse at any point of the segment* $[x_1; x_2]$.

1.3. Asymptotic Behaviour at a Collapse Point: $P(x_0) < 0$

1.3.1. Asymptotic Expansions

If $P(x)$ is negative at least at one point $x_0 \in \mathbb{R}$, formal asymptotic expansions predict existence of two one-parametric families of the solutions for the equation (2.1) collapsing at this point.

Let us construct these asymptotic expansions. We suppose that $P(x_0) = -1$ (this condition can be achieved by a simple renormalisation of the independent variable), denote by $\eta = x - x_0$, and assume that in the vicinity of the point $x = x_0$, the following expansions are valid:

$$Q(x) = Q_0 + Q_1\eta + Q_2\eta^2 \ldots, \quad P(x) = -1 + P_1\eta + P_2\eta^2 + \ldots. \tag{1.13}$$

Substituting these expansions into (2.1), we have

$$u_{\eta\eta} + (Q_0 + Q_1\eta + Q_2\eta^2 \ldots)u + (-1 + P_1\eta + P_2\eta^2 + \ldots)u^3 = 0. \tag{1.14}$$

If a solution of the equation (1.14) collapses at the point $x = x_0$ then it satisfies the following condition, $u(\eta) \to \pm\infty$, when $\eta \to 0$. Let η approaches to zero *from the right*, $\eta > 0$. We make the following variable changes $v(\eta) = \eta u(\eta)$, $\eta = e^{-t}$. It gives

$$v_{tt} + 3v_t + 2v + e^{-2t}Q(t)v + P(t)v^3 = 0. \tag{1.15}$$

Let's determine the main term of the expansion by balancing $2v$ and $-v^3$ terms, we have

$$V_0(t) = \pm\sqrt{2}. \tag{1.16}$$

Now let's define the first order term $V_1(t)$, $v(t) = \pm\sqrt{2} + V_1(t) + o(V_1(t))$. Substituting the last expression into the (1.15), considering expansion for the functions $Q(t)$, $P(t)$, and omitting the terms of order higher than e^{-t}, we obtain

$$V_{1,tt} + 3V_{1,t} - 4V_1 = \mp 2\sqrt{2}e^{-t}, \tag{1.17}$$

that gives $V_1(t) = \pm\frac{\sqrt{2}}{3}e^{-t}$. Second, third, and forth order terms V_n, $n = 2, 3, 4$, can be found in a similar manner. For each term the corresponding equation takes form:

$$V_{n,tt} + 3V_{n,t} - 4V_n = C_n e^{-nt}. \tag{1.18}$$

However, for $n = 2, 3$ solutions of the equation (1.18) are of the form $V_n \sim e^{-nt}$, but in the case $n = 4$, the exponent term in the right hand side coincides with one of the roots of the characteristic polynomial for the differential operator in the left-hand side. In this case solution of the equation (1.18) must be chosen in the form $Ce^{-4t} - A_3 te^{-4t}$. Here C in an arbitrary constant, while A_3 can be determined uniquely from the coefficients of the series expansions for $Q(t)$, $P(t)$. If constant C is fixed, at the further steps of this procedure the corresponding equations are uniquely solvable. One can note that the replacement of $+$ to $-$ in the expression (1.16) leads to the corresponding replacement of the signs for all coefficients A_n, $n = 0, 1, ...$, that is natural due to the invariance of the equation (2.1) with regard to the change $u \to -u$. We have

$$\pm v(t) = \sqrt{2} + A_0 e^{-t} + A_1 e^{-2t} + A_2 e^{-3t} + A_3 \cdot (-t) \cdot e^{-4t} + Ce^{-4t} + \dots . \tag{1.19}$$

Explicit expressions for the $A_0, \dots, A_3$ are:

$$A_0 = \frac{\sqrt{2}}{3} P_1; \tag{1.20}$$

$$A_1 = \frac{\sqrt{2}}{3} P_2 + \frac{\sqrt{2}}{6} Q_0 + \frac{2\sqrt{2}}{9} P_1^2; \tag{1.21}$$

$$A_2 = \frac{2\sqrt{2}}{3} P_2 P_1 + \frac{7\sqrt{2}}{27} P_1^3 + \frac{\sqrt{2}}{6} Q_0 P_1 + \frac{\sqrt{2}}{4} Q_1 + \frac{\sqrt{2}}{2} P_3; \tag{1.22}$$

$$A_3 = -\frac{\sqrt{2}}{6} Q_1 P_1 - \frac{\sqrt{2}}{5} Q_2 - \frac{32\sqrt{2}}{45} P_2 P_1^2 - \frac{3\sqrt{2}}{5} P_3 P_1 - \tag{1.23}$$

$$-\frac{2\sqrt{2}}{15} P_2 Q_0 - \frac{2\sqrt{2}}{15} Q_0 P_1^2 - \frac{2\sqrt{2}}{5} P_4 - \frac{28\sqrt{2}}{135} P_1^4 - \frac{4\sqrt{2}}{15} P_2^2. \tag{1.24}$$

In the other case when $\eta \to 0$ *from the left*, $\eta < 0$, to construct similar expansions one should make the variable changes $v(\eta) = \eta u(\eta)$, $\eta = -e^{-t}$. Expressions for the coefficient A_n remain the same as for $\eta > 0$.

Finally we get an asymptotic expansion for the original solution $u(x)$ for $x \to x_0 \pm 0$:

$$\pm u(x) = \frac{\sqrt{2}}{\eta} + A_0 + A_1 \eta + A_2 \eta^2 + A_3 \eta^3 \ln|\eta| + C\eta^3 + A_4 \eta^4 \ln|\eta| + \dots . \tag{1.25}$$

here $\eta = x - x_0$, $A_0, \dots, A_3$ are determined by the equations (1.20)-(1.24), and all other coefficients A_n, $n > 3$ can be expressed with Q_n, P_n and arbitrary constant C.

Summarizing all above mentioned, one can say that asymptotic expansion (1.25) *predicts the existence* of two one-parametric families of solutions collapsing at the point x_0. These families are connected by the symmetry $u \to -u$. When $x \to x_0$, the solutions from one of these families tends to $+\infty$, while solutions from another family tends to $-\infty$ correspondingly.

1.3.2. Existence of One-Parametric Families of Collapsing Solutions

The possibility of constructing asymptotic expansions (1.25) itself does not prove the existence of one-parametric families of solutions collapsing at point x_0. But at the same time, the following rigorous statement is true.

Proposition 2. *Let Ω be a neighbourhood of the point x_0, $Q(x) \in C^3(\Omega)$ and $P(x) \in C^4(\Omega)$, then there exist two C^1-smooth one-parametric families of solutions for the equation* (2.1) *corresponding to the expansions* (1.25)*, collapsing at the point $x = x_0$ (while approaching from the left, $x < x_0$), and connected by a symmetry $u \to -u$. Each of these families can be parametrized by a free variable $C \in \mathbb{R}$ from the expansions* (1.25)*.*

Proof. By the initial statement the following expansions are valid:

$$Q(x) = Q_0 + Q_1\eta + Q_2\eta^2 + \widetilde{Q}(\eta)\eta^3; \tag{1.26}$$

$$P(x) = -1 + P_1\eta + P_2\eta^2 + P_3\eta^3 + P_4\eta^4 + \widetilde{P}(\eta)\eta^5. \tag{1.27}$$

Here $\eta = x - x_0$, and $\widetilde{Q}, \widetilde{P} \in C(\Omega)$. To prove existence of the family that corresponds to the $+$ sign in (1.25) we make a variable change:

$$u(x) = \frac{\sqrt{2}}{\eta} + A_0 + A_1\eta + A_2\eta^2 + A_3\eta^3 \ln(-\eta) + z(\eta)\eta^3, \tag{1.28}$$

where $z(\eta)$ is a new unknown function. Coefficients $A_0, \ldots, A_3$ are chosen accordingly to the expressions (1.20)-(1.24), so the coefficients at the terms η^{-2}, η^{-1}, η^0, and η are vanish. It's easy to check that direct substitution of the (1.28) into (2.1) shows that for such choice of $A_0, \ldots, A_3$ the following equation for z takes place:

$$z_{\eta\eta} + \frac{6}{\eta} z_\eta + g(\eta, z) = 0, \tag{1.29}$$

where $g(\eta, z)$ is a third order polynomial with respect to z, and $g(\eta, z) \sim \frac{ln(-\eta)}{\eta}$ when $\eta \to -0$ and z is fixed. Variable change $\eta = -e^{-t}$ map the point $\eta = 0$ into $t = +\infty$, and turn equation (1.29) into

$$z_{tt} - 5z_t - f(t, z) = 0. \tag{1.30}$$

Here $f(t, z) \sim te^{-t}$ while $t \to +\infty$. Properties of the function $f(t, z)$ allows us to apply *Lemma on Bounded Solutions* from Appendix A to the equation (1.30). This lemma states that for $t \to +\infty$ all bounded solutions of the equation (1.30) tend to some constant C when $t \to +\infty$, moreover for each $C \in \mathbb{R}$ there exists unique solution that approaches to that constant asymptotically while $t \to +\infty$. Furthermore these solutions form a C^1-smooth family. Finally we can move to the previous equation (1.29), and then to the (2.1) to get the initial statement of the proposition. The existence of the second family of solutions corresponding to the sign "$-$" in (1.25) follows from the invariance of equation (2.1) under the replacement $u \to -u$. □

Similar one-parametric families of collapsing solutions exist from the right side of the point $x = x_0$. The corresponding proof can be performed in the same way.

1.4. All Solutions Are Singular: $P(x) \leq P_0 < 0$, $Q(x) \leq Q_0 < 0$

It turns out that under some assumptions all non-trivial solutions of the equation (2.1) are singular.

Proposition 3. *Let for all $x \in \mathbb{R}$ conditions $P(x) \leq P_0 < 0$, $Q(x) \leq Q_0 < 0$ take place, then all solutions of the equation (2.1) are singular except for the zero one.*

To prove this proposition we prove the following auxiliary lemma first.

Lemma 1. *Let $p, q > 0$ are real constants, then all solutions of equation*

$$v_{xx} - qv - pv^3 = 0, \tag{1.31}$$

are singular except for the zero one.

Proof. Solution to the Cauchy problem for the equation (1.31) with initial conditions $v(x_0) = v_0$, $v_x(x_0) = v_0'$ can be written in an implicit way as:

$$\pm \int\limits_{v_0}^{v} \frac{d\xi}{\sqrt{C + q\xi^2 + \frac{p}{2}\xi^4}} = x - x_0; \quad C \equiv (v_0')^2 - qv_0^2 - \frac{p}{2}v_0^4. \tag{1.32}$$

Choice of the sign in the left hand-side depends on the initial conditions and the value of x. Integral in the left hand-side of the equality (1.32) converges when $v \to \infty$, and hence there exist a value x^*, defined as

$$x^* = x_0 \int\limits_{v_0}^{\infty} \frac{d\xi}{\sqrt{C + q\xi^2 + \frac{p}{2}\xi^4}}, \tag{1.33}$$

and $v(x)$ goes to infinity while x approaches to the x^* So a solution $v(x)$ with arbitrary non-zero initial conditions is singular, lemma is proven. □

Now we can prove the Proposition 3.

Proof of the Proposition 3. We use a so-called *Comparison Lemma* from [6, Appendix C]. Consider the equation

$$v_{xx} + Q_0 v + P_0 v^3 = 0. \tag{1.34}$$

We introduce the denotations

$$g(x, \xi) \quad = -Q(x)\xi - P(x)\xi^3; \tag{1.35}$$

$$f(x, \xi) = f(\xi) \quad = -Q_0\xi - P_0\xi^3. \tag{1.36}$$

Now we apply Comparison Lemma to the following pair of equations:

$$u_{xx} = g(x, u); \tag{1.37}$$

$$v_{xx} = f(x, v). \tag{1.38}$$

In the domain $D_+ = \{x \in \mathbb{R}, \xi \in (0; +\infty)\}$ we have $f(x, \xi) \leq g(x, \xi)$. Let $\widetilde{u}(x)$ be a solution to the Cauchy problem for the equation (1.37) with initial conditions

$u(x_0) = u_0$, $u_x(x_0) = u'_0$. Chose the initial conditions for the Cauchy problem for the equation (1.38) as follows: $v(x_0) = u(x_0) = u_0$, $v_x(x_0) = u_x(x_0) = u'_0$; let $\widetilde{v}(x)$ is a solution for that second problem. Let $u_0 > 0$, then one of the two cases takes place.

(i) $u'_0 \geq 0$. Function $\widetilde{v}(x)$ increases monotonically; this fact can be easily established from the phase portrait of the equation (1.38). Solution $\widetilde{u}(x)$ limits solution $\widetilde{v}(x)$ from above, which is singular. It follows from the Comparison Lemma that solution $\widetilde{u}(x)$ is also singular.

(ii) $u'_0 < 0$. We make a variable change $= -x$. In that case solution $\widetilde{v}(\widetilde{x})$ also increases monotonically, and since $\widetilde{u}(\widetilde{x})$ limits $\widetilde{v}(\widetilde{x})$ from above, $\widetilde{u}(\widetilde{x})$ is singular by the Comparison Lemma, hence $\widetilde{u}(x)$ is also singular.

Similarly in the domain $D_- = \{x \in \mathbb{R}, \xi \in (-\infty; 0)\}$, the inequality $f(x, \xi) \geq g(x, \xi)$ holds. One can prove in the same manner that in the domain D_- solution $u(x)$ is also singular. □

1.5. Summary

Our main findings on regular and singular solutions for the stationary states equation (2.1) are summarised within Table 1.1. All these results were published by us in [7]. Our further findings are focused on the case when $P(x)$ changes its sign along the x. In the next chapter we describe a so-called *singular solution elimination method* which allow us under some additional assumptions classify all regular stationary states solution for the equation (2.1) within the symbolic dynamics framework.

$P(x)$	$Q(x)$	
$P(x) > 0$	—	All the solutions can be continued to the whole real line, singular solutions are absent (Proposition 1).
$P(x) < 0$ at least at one point $x = x_0$	—	There exists a pair of one-parametrical family of solutions collapsing at point $x = x_0$ and related by the symmetry $u \to -u$ (Proposition 2).
$P(x) < 0$	$Q(x) < 0$	All solutions are singular except for the zero one (Proposition 3).
$P(x)$ changes sign along $\mathbb{R}$	—	Singularity is a common behaviour of solutions. That fact allows us under some additional assumption apply so-called *singular solution elimination method* and classify all remaining regular solutions in terms of symbolic dynamics. We reveal this method and its application in the Chapter 2.

Table 1.1. Summary of the results for the Chapter 1.

Chapter 2

Stationary States Classification Within Symbolic Dynamics Framework

2.1. Objections

In this chapter we describe an approach that is used further in order to classify all stationary state of one-dimensional GPE that are described by the stationary states equation:

$$u_{xx} + Q(x)u + P(x)u^3 = 0. \tag{2.1}$$

Here and after we assume $Q(x)$, $P(x)$ to be periodic functions of the same period L: $Q(x+L) = Q(x)$, $P(x+L) = P(x)$ which is quite typical for different physical applications. We also assume functions $Q(x)$, $P(x)$ to be at least piece-wise continuously differentiable. That allows us to split the whole real axis $\mathbb{R}$ into separate intervals where the corresponding Cauchy problem correctly defined and a solution for any initial conditions exists and is unique within each such interval.

Our classification approach is based on the technique proposed in the work [8]. In [8] authors show that presence of a large number of singular solutions families allows to classify all remaining bounded solutions within a symbolic dynamics framework. That leads us to another important requirement, function $P(x)$ must *changes its sign along the period* L. As we saw in the previous chapter such fact guarantees the existence of singular solution families that in its turn becomes a foundation of the technique and makes the announced approach even possible.

Goal of this chapter is to provide a stationary states classification framework and point out the boundaries of its application. Core idea is the following. We define a Poincaré map $\mathcal{P}$ for the stationary states equation (2.1). Since function $P(x)$ alternates its sing, Poincaré map $\mathcal{P}$ and an inverse map $\mathcal{P}^{-1}$ cannot be defined on the whole phase plane, instead they are defined on some phase plane subset.

Studying the domains of maps $\mathcal{P}$, $\mathcal{P}^{-1}$ is a crucial aspect of the proposed approach. We determine conditions which allow to conclude that Poincaré map acts on the defined set as a kind of the *horseshoe map* [9, Chapter 5]. Domains of the higher order maps $\mathcal{P}^2$, $\mathcal{P}^3, \ldots$ and domains of the inverse maps $\mathcal{P}^{-2}$, $\mathcal{P}^{-3}, \ldots$ can be obtained by the refinement of the initial area. Finally if some conditions are met and we can conclude that there exists one-to-one correspondence between all bounded solution of the equation (2.1) and a points set on the phase plane which is a result of the above mentioned refinement. That is what we call singular solution elimination method.

The presence of the horseshoe map structure allows us for each bounded solution uniquely specify a bi-infinite symbolic sequence over some alphabet (finite or even infinite) and such correspondence is also bijective. We refer to the result bi-infinite sequence as *solution code* and the overall process as *solutions coding.* Such coding, if possible, provides a complete picture of the bounded solutions family for the equation (2.1) that can be highly demanded in different physical applications which involves Gross-Pitaevskii equation with both periodic potential and periodic pseudopotential.

2.2. Geometry of the Poincaré Map

First of all let's introduce several definitions which describe basic structures and their relationships that are in the core of the overall further narration.

2.2.1. Poincaré Map

Since we consider functions $Q(x)$, $P(x)$ to be L-periodic let's introduce the Poincaré map associated with the period L of the equation (2.1). Define the Poincaré map $\mathcal{P} : \mathbb{R}^2 \to \mathbb{R}^2$ in the following manner:

$$\mathcal{P}\begin{pmatrix} u_0 \\ u_0' \end{pmatrix} = \begin{pmatrix} u_L \\ u_L' \end{pmatrix}, \tag{2.2}$$

where $u_L = u(L)$, $u'_L = u'(L)$, and $u(x)$ is a solution of the equation (2.1) with initial conditions $u(0) = u_0$, $u'(0) = u'_0$. Poincaré map by itself is an *area-preserving diffeomorphism*. Obviously, and as we mentioned above, Poincaré map $\mathcal{P}$ and its inverse $\mathcal{P}^{-1}$ may not be defined on the whole plane (u, u') of initial conditions. Denote by $\mathscr{U}_L^+$ the domain of the map $\mathcal{P}$, and denote by $\mathscr{U}_L^-$ the domain of the map $\mathcal{P}^{-1}$ correspondingly. Also define a set $\mathscr{U}_L$ as an intersection of the two above mentioned sets: $\mathscr{U}_L = \mathscr{U}_L^+ \cap \mathscr{U}_L^-$.

It obviously follows from the definitions of $\mathscr{U}_L^\pm$ that $\mathcal{P}(\mathscr{U}_L^+) = \mathscr{U}_L^-$. Indeed any point $\mathbf{p} \in \mathscr{U}_L^+$ has $\mathcal{P}$-image $\mathbf{q}$. Then $\mathbf{q}$ has $\mathcal{P}$-pre-image, therefore $\mathbf{q} \in \mathscr{U}_L^-$. On the other hand if $\mathbf{q} \in \mathscr{U}_L^-$ then $\mathbf{q}$ has $\mathcal{P}$-pre-image $\mathbf{p}$. Therefore $\mathbf{p}$ has $\mathcal{P}$-image and hence $\mathbf{p} \in \mathscr{U}_L^+$. Backward statement $\mathcal{P}^{-1}(\mathscr{U}_L^-) = \mathscr{U}_L^+$ is also valid.

We also note here that symmetry in equation (2.1) naturally produces symmetry in $\mathcal{U}_L^\pm$ sets. For example we can prove the following important statement.

Proposition 4. *Let functions $Q(x)$, $P(x)$ are even, then*

$$\mathcal{P}(\mathscr{U}_L^+) = I(\mathscr{U}_L^+); \tag{2.3}$$

$$\mathcal{P}^{-1}(\mathscr{U}_L^-) = I(\mathscr{U}_L^-), \tag{2.4}$$

where map I is a reflection with respect to the u' axis.

Proof. Let's prove statement (2.3). Consider a point $\mathbf{q} \in \mathcal{P}(\mathscr{U}_L^+)$. By definition of $\mathscr{U}_L^+$ set there is a point $\mathbf{p} = (u_0, u'_0) \in \mathscr{U}_L^+$, such that there exists a solution $u(x)$ of (2.1) with initial conditions $u(0) = u_0$, $u'(0) = u'_0$, and $\mathbf{q} = (u(L), u'(L))$. Denote by $\widetilde{\mathbf{p}}$ a reflection $I(\mathbf{p})$, $\widetilde{\mathbf{p}} = (-u_0, u'_0)$. Next we note that equation (2.1) along with the proposition assumptions on functions $Q(x)$, $P(x)$ admits the variables change $\widetilde{u} = -u$, $\widetilde{x} = -x$ and the form of (2.1) remains exactly the same. It means that $\widetilde{u}(\widetilde{x})$ is also a solution of (2.1) with initial conditions $\widetilde{u}(0) = -u_0$, $\widetilde{u}'(0) = u'_0$. It follows from the introduced variables change that $\widetilde{u}(-L) = -u(L) = -u_L$ and $\widetilde{u}'(-L) = u'(L) = u'_L$. Denote this new point by $\widetilde{\mathbf{q}} = (\widetilde{u}(-L), \widetilde{u}'(-L))$. By definition of $\mathcal{P}$ map, $\widetilde{\mathbf{q}} = \mathcal{P}^{-1}(\widetilde{\mathbf{p}})$ and hence $\widetilde{\mathbf{q}} \in \mathscr{U}_L^+$. On the other hand $\widetilde{\mathbf{q}} = (-u_L, u'_L) = I(\mathbf{q})$.

Finally from $I(\mathbf{q}) \in \mathscr{U}_L^+$ we get $\mathbf{q} \in I(\mathscr{U}_L^+)$. It's also pretty straightforward to check backward statement $\mathbf{q} \in I(\mathscr{U}_L^+) \Rightarrow \mathbf{q} \in \mathcal{P}(\mathscr{U}_L^+)$ and eventually prove the equality (2.3). Statement (2.4) can be proven in an identical manner. $\square$

If the conditions of Proposition 4 are met one can conclude that $I(\mathscr{U}_L^+) = \mathscr{U}_L^-$ and $I(\mathscr{U}_L^-) = \mathscr{U}_L^+$, so the above mentioned sets are connected with each other with a reflection with respect to the u' axis.

Definition 1. *Define an* **orbit** *as a sequence of points* $\{\mathbf{p}_n\}$, $\mathbf{p}_n \in \mathbb{R}^2$ *such that* $\mathcal{P}(\mathbf{p}_n) = \mathbf{p}_{n+1}$.

Let $\mathbf{p}_0$ be a starting point. Since $\mathcal{P}$ is defined only on the $\mathscr{U}_L^+$ set, the next point $\mathbf{p}_1$ of the orbit exists only if $\mathbf{p}_0 \in \mathscr{U}_L^+$. Moreover for $n > 0$ points $\mathbf{p}_n$ are consecutive $\mathcal{P}$-iterations of the initial point $\mathbf{p}_0$. If at k-th iteration $\mathcal{P}^k(\mathbf{p}_0)$ leaves the $\mathscr{U}_L^+$ set then the orbit cannot be defined for $n > k$. Similarly for $n < 0$ points $\mathbf{p}_n$ are consecutive $\mathcal{P}^{-1}$-iterations of $\mathbf{p}_0$. Since the $\mathcal{P}^{-1}$ map defined only on the $\mathscr{U}_L^-$ set the iterations may stop after a finite number of steps. As a consequence not all orbits are bi-infinite. But bi-infinite orbits are also exists. For example one can easily specify the bi-infinite orbit of zero points that trivially satisfies the equation (2.1) and corresponds to its zero solution $u(x) \equiv 0$.

Another interesting observation comes from Proposition 1. If the function $P(x) > 0$ for all $x \in \mathbb{R}$ then all the orbits for the equation (2.1) are bi-infinite. From that point of view the case when $P(x)$ changes its sing becomes interesting. According to Proposition 2 points where $P(x) < 0$ form the families of collapsing solutions. Such families at their turn sift the set of bi-infinite orbits. It becomes highly desired, and we'll require it further, that the defined set $\mathscr{U}_L$, produced by the Poincaré map $\mathcal{P}$, represents a so-called *island set* [8] (it will be defined soon). Looking ahead, such structure along with additional properties clearly reveals the horseshoe structure and allows us to formulate and prove all the essential theorems and describe the set of remaining bi-infinite orbits.

2.2.2. Islands Set

Definition 2. *Let $\gamma > 0$ is fixed. A continuous function $f(x) : \Delta \to \mathbb{R}^2$, $\Delta = [a, b]$ is called* **γ-Lipschitz** *function if $\forall x_1, x_2 \in \Delta$ the following inequality holds:*

$$|f(x_1) - f(x_2)| \leq \gamma |x_1 - x_2|. \tag{2.5}$$

Definition 3. *We call* **island** *an open curvilinear quadrangle $D \subset \mathbb{R}^2$ on the phase plane (u, u') formed by two pairs of nonintersecting monotonic curves $\alpha^{\pm}$, $\beta^{\pm}$, moreover:*

- *curves $\alpha^{\pm}$ are graphs of monotonic γ-Lipschitz functions $u' = h_{\pm}(u)$, and a solution of the equation (2.1) with initial conditions $(u_0, u_0') \in \alpha^{\pm}$ collapses at the point $x = -L$;*
- *curves $\beta^{\pm}$ are graphs of monotonic γ-Lipschitz functions $u = v_{\pm}(u')$, and a solution of the equation (2.1) with initial conditions $(u_0, u_0') \in \beta^{\pm}$ collapses at the point $x = +L$;*
- *if the functions $h_{\pm}(u)$ are increasing then $v_{\pm}(u')$ are decreasing, and vice versa, if functions $h_{\pm}(u)$ are decreasing then $v_{\pm}(u')$ are increasing respectively.*

Remark 1. *For convenience hereinafter by monotonically increasing / decreasing function we mean a function that satisfy non-strict inequalities. We call function $f(x)$ monotonically increasing if for $x_1 < x_2$, $f(x_1) \leq f(x_2)$, and monotonically decreasing if $f(x_1) \geq f(x_2)$.*

To emphasise the fact that Lipschitz constant γ must be predefined we also refer to the island as **γ-island**. We also say that points from the island boundaries are *mapped to infinity* by $\mathcal{P}$ ($\beta^{\pm}$ boundaries) or $\mathcal{P}^{-1}$ ($\alpha^{\pm}$ boundaries), since the corresponding solution to the Cauchy problem with initial conditions in that points collapse exactly in the points $x = \pm L$.

Remark 2. *If D is a γ_1-island and $\gamma_2 > \gamma_1$ then D also is a γ_2-island.*

In our definition of island we explicitly specify its connection with initial equation (2.1) and collapses of its solutions. Further we'll see that such connection naturally comes from the dynamics of the $\mathcal{P}$ map for equation of such type.

Remark 3. *Solution of the Cauchy problem for the initial conditions at the intersections of the $\alpha^{\pm}$, $\beta^{\pm}$ curves collapse both in $x = +L$ and $x = -L$ points.*

Definition 4. *Let S be a finite or a countable set of indices. Define* **island set** *as a set $\mathcal{D} = \bigcup_{i \in S} D_i$ that represents finite or countable union of disjoint islands.*

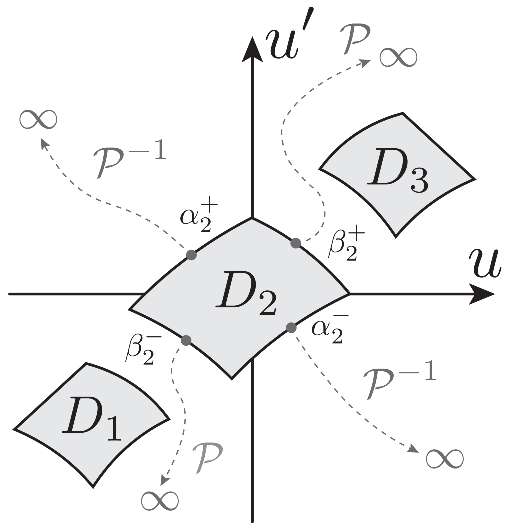

Figure 2.1. Hypothetical example of an island set $\mathcal{D} = \bigcup_{i \in \{1,2,3\}} D_i$ on a plane of initial conditions for the equation (2.1). Boundaries of each component are mapped to the infinity by the $\mathcal{P}$ and $\mathcal{P}^{-1}$ maps (solution of the corresponding Cauchy problem is collapses).

2.2.3. Curves and Strips

Move on to the definition of h,v-curves and h,v-strips. Such curves and strips along with theirs transformations are the object of our attentive study.

Definition 5. *Let D be an island bounded by curves $\alpha^{\pm}$, $\beta^{\pm}$. Consider a curve α that connects the opposite sides $\beta^{\pm}$ of the island D. We call such curve* **h-curve** *if it represents a graph of a monotonic γ-Lipschitz function $u' = h(u)$ and its monotonicity type coincide with the functions $u' = h_{\pm}(u)$ that correspond to the $\alpha^{\pm}$*

boundaries of the island D. We also call **h-strip** *an open subset of the island D bounded by two* h*-curves.*

Definition 6. *Similarly consider a curve β that connects opposite sides $\alpha^{\pm}$ of an island D. We call it* **v-curve** *if it represents a graph of a monotonic γ-Lipschitz function $u = v(u')$ and its monotonicity type coincide with the functions $u = v_{\pm}(u')$ that correspond to the $\beta^{\pm}$ boundaries of the island D. In a like manner we call* **v-strip** *an open subset of the island D bounded by two* v*-curves.*

Remark 4. *Island by itself represents a limit case of the h and v strips simultaneously.*

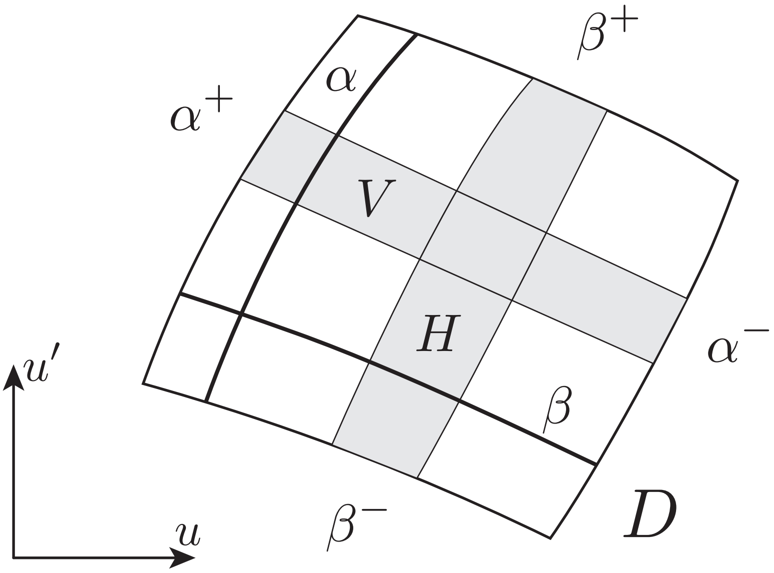

Figure 2.2. An islands D bounded by curves $\alpha^{\pm}$, $\beta^{\pm}$; h-curve α, v-curve β, and two strips: h-strip H and v-strip V.

All above introduced definitions are illustrated on Figures 2.1 and 2.2. At last let's define one additional property of island set along with $\mathcal{P}$, $\mathcal{P}^{-1}$ maps.

Definition 7. *Let $\mathcal{D}$ be an island set formed by the domains of the $\mathcal{P}$ and $\mathcal{P}^{-1}$ maps that act on this set. Consider two islands $D_1, D_2 \in \mathcal{D}$. We call the island D_2* **forward-reachable** *from the island D_1 if for any* h*-curve $\alpha \in D_1$ with endpoints lying on the opposite boundaries $\beta_1^{\pm}$ of the island D_1 the intersection $\mathcal{P}(\alpha) \cap D_2$ is not empty. On the other hand we call the island D_2* **backward-reachable**

from the island D_1 if for any v*-curve $\beta \in D_1$ with endpoints lying on the opposite boundaries $\alpha_1^{\pm}$ of the island D_1 the intersection $\mathcal{P}^{-1}(\beta) \cap D_2$ is not empty. Finally we call the island D_2* **reachable** *from the D_1 if it satisfies both forward and backward reachability.*

Remark 5. *If an island D_2 is forward-reachable from D_1 then D_1 is backward-reachable from D_2 and vice versa.*

Definition 8. *We call an island set $\mathcal{D} = \bigcup_{i \in S} D_i$* **complete** *if for any i, j island D_i is reachable from D_j.*

2.2.4. Thickness of Strips

Next we'll also need a definition of the strips thickness. Let an h-strip H lies inside an island D and is bounded by h-curves α^+ and α^-. Consider graphs of that curves as a functions of u: $u' = h_{\pm}(u)$. By the definition $h_{\pm}(u)$ are γ-Lipschitz function. Denote by $\Delta^{\pm}$ their domains. Obviously due to the geometric properties of an island domains $\Delta^{\pm}$ do not coincide except the case when the opposite boundaries $\beta^{\pm}$ lying on the corresponding boundaries of the island D are vertical straight lines. Let $\Delta^+ = [u_0^+; u_1^+]$, $\Delta^- = [u_0^-; u_1^-]$, consider new domain $\Delta = \Delta^+ \cap \Delta^-$ and define functions $\widetilde{h}_{\pm}(u)$ on the new domain Δ as follows:

$$\widetilde{h}_{\pm}(u) = \begin{cases} h_{\pm}(u_0^{\pm}) & u < u_0^{\pm}; \\ h_{\pm}(u) & u \in \Delta^{\pm}; \\ h_{\pm}(u_1^{\pm}) & u > u_1^{\pm}. \end{cases} \tag{2.6}$$

Since $h_{\pm}$ are γ-Lipschitz functions the new functions $\widetilde{h}_{\pm}$ are also γ-Lipschitz on the whole domain Δ. Denote by $\widetilde{\alpha}^{\pm}$ the resulted curves formed by the graphs $\widetilde{h}_{\pm}(u)$.

Definition 9. *By the* **thickness** *of an h-strip H, denoted $d_{\mathrm{h}}(H)$, we mean the distance between curves $\widetilde{\alpha}^{\pm}$ in C-norm, i.e.*

$$d_{\mathrm{h}}(H) = d(\widetilde{\alpha}^+, \widetilde{\alpha}^-) = \max_{u \in \Delta} |\widetilde{h}_+(u) - \widetilde{h}_-(u)|. \tag{2.7}$$

Remark 6. *For two* h*-strips* H_1*,* H_2 *the following statement is valid:* $H_2 \subseteq H_1 \Rightarrow \Delta_2 \subseteq \Delta_1$ *and* $d_{\mathrm{h}}(H_2) \leq d_{\mathrm{h}}(H_1)$*.*

Definition 10. *Let maximum of the expression* (2.7) *is reached at a point* u_**, i.e.*

$$u_* = \arg\max_{u \in \Delta} |\widetilde{h}_+(u) - \widetilde{h}_-(u)|. \tag{2.8}$$

We call an h*-strip* H **well-measurable** *if* $u_* \in \Delta^+ \cap \Delta^-$*.*

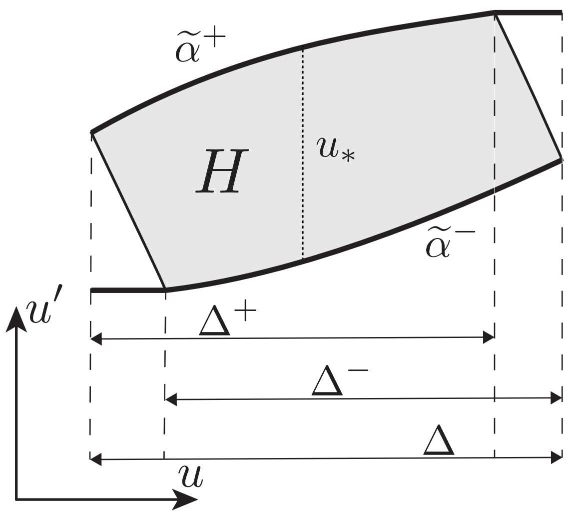

Figure 2.3. An illustration to the definition of an h-strip thickness. Strip H is *well-measurable* in a sense of Definition 10. Curves $\widetilde{\alpha}^{\pm}$ are continuations of the initial h-strip borders to the whole Δ; u_* is a point of maximum of the expression (2.7).

Proposition 5. *For the* h*-strip* H *the following statement is valid:*

$$\Delta^+ \cap \Delta^- \neq \varnothing \Rightarrow u_* \in \Delta^+ \cap \Delta^-, \tag{2.9}$$

i.e. an h*-strip is well-measurable if domains of its border functions have at least one common point.*

Proof. Trivially follows from the monotonicity of the h-strip borders α^+ and α^-. □

In a similar way we define thickness of v-strips. Let an v-strip V lies inside an island D and is bounded by v-curves β^+ and β^-. Consider this curves as a functions of u': $u = v_\pm(u')$. Denote domains of these functions by $\Delta^\pm$. Continue functions $v_\pm(u')$ to the whole interval $\Delta = \Delta^+ \cap \Delta^-$ in the same way as for h-strips, see (2.6), and introduce new functions $\widetilde{v}_\pm(u')$ and curves $\widetilde{\beta}^\pm$.

Definition 11. *By the* **thickness** *of an v-strip V, denoted $d_{\mathrm{v}}(V)$, we mean the distance between curves $\widetilde{\beta}^\pm$ in C-norm, i.e.*

$$d_{\mathrm{v}}(V) = d(\widetilde{\beta}^+, \widetilde{\beta}^-) = \max_{u' \in \Delta} |\widetilde{v}_+(u') - \widetilde{v}_-(u')|. \tag{2.10}$$

The definition of *well-measurable* v-strip is introduced in a same way. The remark and the proposition above remain valid for the v-strips as well. Note that thickness of h-strip is measured in a vertical direction, and thickness of v-strip is measured in a horizontal direction. If a strip is well-measurable then its thickness is measured in a direction along the straight line that connects points from the opposite side of the strip. This concept will be useful for us during the proof of a theorem about h,v-strips mapping which are formulated in Appendix C.

2.3. Poincaré Map Domains for Piecewise Periodic Pseudopotential

Let's demonstrate how the definitions introduced above work all together. For that purpose consider a simple form of one-dimensional GPE with periodically modulated pseudopotential

$$i\Psi_t + \Psi_{xx} + \eta(x)|\Psi|^2\Psi = 0, \tag{2.11}$$

where $\eta(x)$ is a periodic piecewise constant function of the period $L = L_* + L_0$:

$$\eta(x) = \begin{cases} -1, & x \in [0; L_*]; \\ +1, & x \in [L_*; L_* + L_0], \end{cases} \tag{2.12}$$

This equation is obtained from the initial equation (1) where we put $P(x) = \eta(x)$

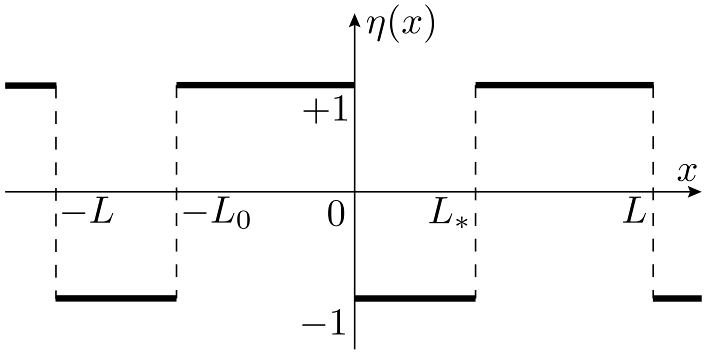

Figure 2.4. ...

and the ordinary potential $U(x)$ is considered to be negligible or even absent, $U(x) \equiv 0$. Again we consider stationary solutions of the form $\Psi(t,x) = u(x)e^{-i\omega t}$, $\omega \in \mathbb{R}$, where function $u(x)$ satisfies the equation

$$u_{xx} - \omega u + \eta(x)u^3 = 0. \tag{2.13}$$

In order to make things even simpler for our demonstration let's also assume $\omega = 1$.

Since pseudopotential is a piecewise constant function that has only two different values on the period L we can split the period into two regions and consider two different regimes of the equation (2.13). In each region the stationary states equation has a familiar form of conservative Duffing equation:

$$u_{xx} - u - u^3 = 0, \quad x \in [0; L_*]; \tag{2.14}$$

$$u_{xx} - u + u^3 = 0, \quad x \in [L_*; L_* + L_0]. \tag{2.15}$$

Each of the equations (2.14), (2.15) can be solved explicitly through Jacobi elliptic functions. Exact solutions are given in Appendix **??**.

Equation (2.14) has a first integral of the form:

$$H_* = u_x^2 - u^2 - \frac{1}{2}u^4. \tag{2.16}$$

The phase portrait of the equation (2.14) is presented on Figure 2.5 (a). Any trajectory on the phase plane corresponds to some value of H_*. Level $H_* = 0$ corresponds to the equilibrium state $(0,0)$, and four separatrices connected to it. Two of the separatrices $\gamma_{1,2}^+$ enter the zero equilibrium as x approaches $+\infty$. We

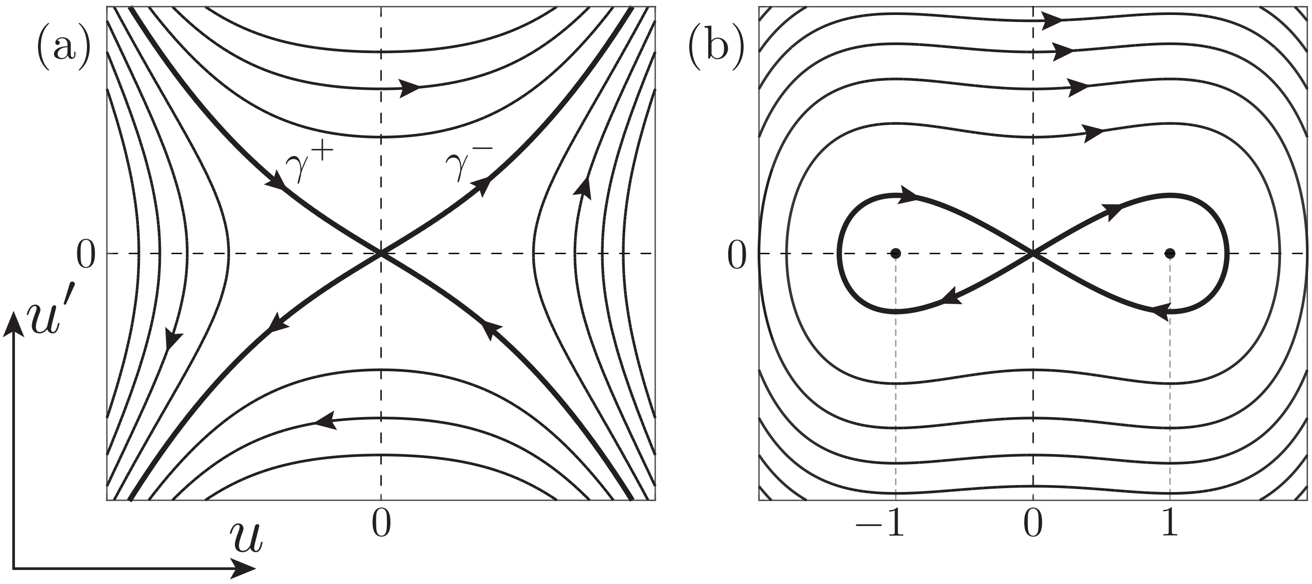

Figure 2.5. Phase portraits for the different regimes of stationary states equation (2.13) with piecewise pseudopotential (2.12). Panel (a) represents a phase portrait for the equation (2.14), curves $\gamma^{\pm}$ correspond to the separatrices which enter the equilibrium point $(0,0)$ as x approaches $\pm\infty$. Panel (b) depicts a phase portrait for the equation (2.15).

denote them along with the point $(0,0)$ by a curve γ^+. Another two separatrices $\gamma^-_{1,2}$ enter the zero equilibrium as x approaches $-\infty$. Along with the point $(0,0)$ we denote them by a curve γ^- correspondingly. Result curves $\gamma^{\pm}$ satisfy equations

$$u' = \pm\frac{u}{\sqrt{2}}\sqrt{2+u^2}. \tag{2.17}$$

It follows from the exact form of the solutions of the equation (2.14) that all of them, except for the zero one, are singular. It means that a solution for a Cauchy problem with initial conditions $u(0) = u_0$, $u'(0) = u'_0$ (u_0 and u'_0 not equals zero simultaneously) tends to infinity while x approaches some finite point both to the left and to the right of $x = 0$. We say that a solution for the equation (2.14) has a *finite domain* if $H_* \neq 0$. That's why we mark a corresponding period part L_* with a symbol "$*$", since the solutions are tend to run out the origin of the phase plane.

The first integral of equation (2.15) is

$$H_0 = u_x^2 - u^2 + \frac{1}{2}u^4. \tag{2.18}$$

Phase portrait for equation (2.15) is given on Figure 2.5 (b). It has two center equilibrium points $(\pm 1, 0)$ and one hyperbolic equilibrium point $(0,0)$. Separatrix loops correspond to the localized solutions

$$u(x) = \pm\frac{\sqrt{2}}{\cosh x}. \tag{2.19}$$

The aria inside the separatrix loops is filled by closed orbits of periodic solutions with nonzero mean. All other orbits turn around the origin and correspond to solutions with zero mean. That's why we mark a corresponding period part L_0 with a symbol "0", since it looks like a little curve circle.

2.3.1. General Propositions on the $\mathscr{U}_L^{\pm}$ Sets for Piecewise Pseudopotential

Let's move on to the consideration of the $\mathscr{U}_L^{\pm}$ sets for the equation (2.13). Recall that we decided to split the period L into two parts $[0; L_*]$ and $[L_*; L_* + L_0]$. From that perspective let's consider a decomposition of the Poincaré map $\mathcal{P} = \mathcal{P}_0\mathcal{P}_*$, where maps associated with corresponding parts of the overall period L are defined in a similar manner as the initial Poincaré map $\mathcal{P}$ itself (2.2). Map $\mathcal{P}_*$ map a point (u_0, u_0') to $(u(L_*), u'(L_*))$ where $u(x)$, $x \in [0; L_*]$ is a solution of Eq. (2.14) with initial conditions $u(0) = u_0$, $u'(0) = u_0'$. Similarly map $\mathcal{P}_0$ map a point (u_0, u_0') to $(u(L), u'(L))$ where $u(x)$, $x \in [L_*; L]$ is a solution of Eq. (2.15) with initial conditions $u(L_*) = u_0$, $u'(L_*) = u_0'$.

Note that $\mathcal{P}_*$ cannot be defined everywhere. We denote by $\mathscr{U}_{L_*}^+$ a domain of the map $\mathcal{P}_*$. Due to the fact that all solutions of the equation (2.15) are regular, domain of the overall Poincaré map $\mathcal{P}$ coincide with the domain of $\mathcal{P}_*$ map, i.e. $\mathscr{U}_L^+ = \mathscr{U}_{L_*}^+$. For the equation (2.13) it can be written as follows:

$$\mathscr{U}_L^+ = \mathrm{dom}(\mathcal{P}) = \mathrm{dom}(\mathcal{P}_0\mathcal{P}_*) = \mathrm{dom}(\mathcal{P}_*) \equiv \mathscr{U}_{L_*}^+. \tag{2.20}$$

It's easy to note several other properties of the $\mathscr{U}_{L_*}^+$ set. Since the phase portrait for Eq. (2.14) is symmetric with respect to the origin, $\mathscr{U}_{L_*}^+$ is also symmetric with respect to the origin. Two separatrices that correspond to the curve γ^+ are tend to zero equilibrium as $x \to +\infty$. It means that for any initial data posed at γ^+ and for any L_* the map $\mathcal{P}_*$ is correctly defined, i.e. $\gamma^+ \in \mathscr{U}^+_{L_*}$. Another property of $\mathscr{U}^+_{L_*}$ directly follows from Proposition 4:

$$\mathcal{P}_*(\mathscr{U}^+_{L_*}) = I(\mathscr{U}^+_{L_*}) = \mathscr{U}^-_{L_*}. \tag{2.21}$$

Move on to the $\mathscr{U}^-_{L_*}$ set for equation (2.14). Since $\mathscr{U}^-_{L_*}$ is a reflection of $\mathscr{U}^+_{L_*}$ set with respect to the u' axis, it inherits its symmetry properties. Set $\mathscr{U}^-_{L_*}$ also contains curve γ^- that corresponds to another two separatrices $\gamma^-_{1,2}$ of equation (2.14). Consider the second map $\mathcal{P}_0$ of the decomposition. As we mentioned above $\mathcal{P}_0$ correctly defined on the whole $\mathscr{U}^-_{L_*}$. If so, it's interesting to figure out how this map transform separatrices curve γ^-. It turns out that the image $\mathcal{P}_0(\gamma^-)$ has a spiral-like structure and intersects the curve γ^+ infinitely many times. The following proposition can be proved.

Proposition 6. *$\mathcal{P}_0$-image of the curve γ^- intersects γ^+ infinitely many times at the points $\{0\} \cup u_{\pm n}$,*

$$u_{\pm n} = \pm\frac{2x_{n-1}}{\sqrt[4]{2}L_0} + \mathcal{O}\left(H_0^{-1/4}\right), \ n \in \mathbb{N}, \tag{2.22}$$

as $H_0 \to \infty$, x_n are determined as

$$x_n = \mathrm{cn}^{-1}\left(2^{-1/4}, k_0\right) + K(k_0)n, \tag{2.23}$$

where $K(k)$ is the complete elliptic integral of the first kind, and $k_0 = 1/\sqrt{2}$.

Proof. First of all, point $(0,0)$ belongs to the intersection $\mathcal{P}_0(\gamma^-) \cap \gamma^+$ since it's a stable fixed point of equation (2.15) and the $\mathcal{P}_0$ map.

Next we note that all the intersections $\mathcal{P}_0(\gamma^-) \cap \gamma^+$ occur outside of the separatrix loops of (2.15) and correspond to zero mean solutions of (2.15). This obviously follows from that fact that γ^+ lies outside of the loops both from left and right of u' axis (depicted on Fig. 2.6 (a)).

Prove the formula for points from the right side of u' axis, u_{+n}. Such points corresponds to the γ_2^+ separatrix of equation (2.14), see Figure 2.6. Result points

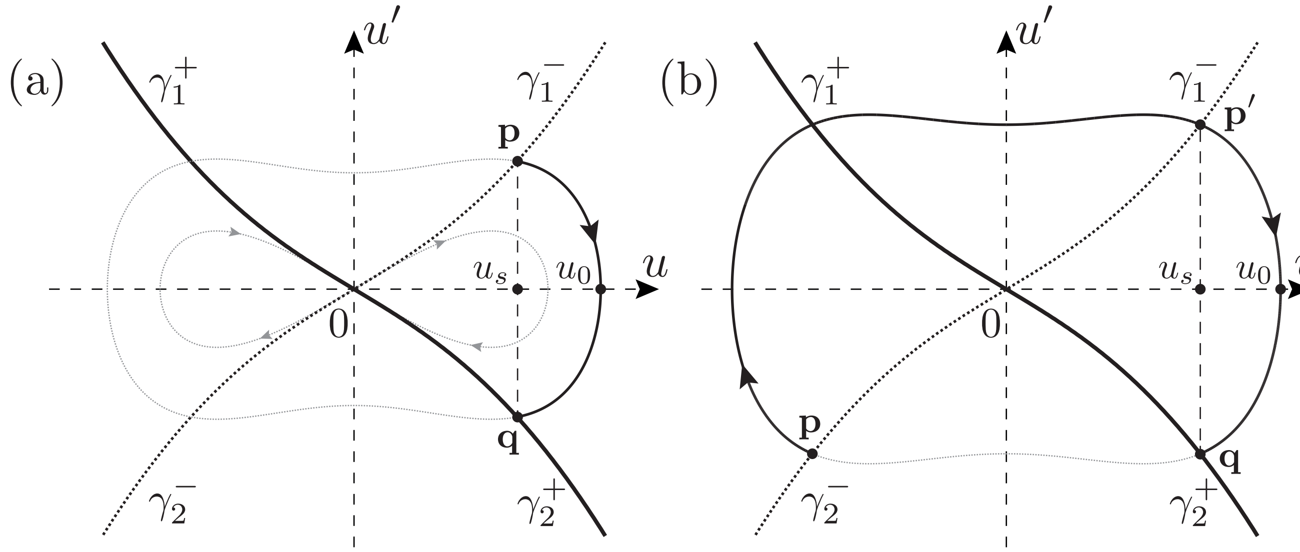

Figure 2.6. Illustration for the proof of Proposition 6.

of intersections $\mathcal{P}_0(\gamma^-) \cap \gamma_2^+$ can be divided into two groups: $\mathcal{P}_0(\gamma_1^-) \cap \gamma_2^+$ and $\mathcal{P}_0(\gamma_2^-) \cap \gamma_2^+$.

Consider points from the first group. Let a point $\mathbf{q}$ belongs to the intersection $\mathcal{P}_0(\gamma_1^-) \cap \gamma_2^+$. Then there exists a point $\mathbf{p} = (u_s, u_s') \in \gamma_1^-$ such that $\mathcal{P}_0(\mathbf{p}) \in \gamma_2^+$. Due to the symmetries of the phase portraits for equations (2.14) and (2.15), $\mathbf{q} = (u_s, -u_s')$, see Figure 2.6 (a). Consider a phase trajectory of (2.15) that lies outside of separatrix loop and connects points $\mathbf{p}$ and $\mathbf{q}$. According to Appendix B exact form of the solution is

$$u(x) = x_0 \mathrm{cn}\left(\sqrt{x_0^2 - 1}x + x_1, k\right), \tag{2.24}$$

where k is elliptic modulus, $k = \dfrac{1}{\sqrt{2}} \dfrac{x_0}{\sqrt{x_0^2 - 1}}$, and x_0, x_1 are constants that can be determined by initial conditions $(u(0), u'(0)) = \mathbf{p}$.

Next let's introduce an x variable shift $x \to x - L_0/2$. Equation (2.24) persists its form but now $u(0) = u_0$, $u_0 > 0$, and $u'(0) = 0$. That allows us to determine constants x_0, x_1: $x_0 = u_0$, $x_1 = 0$. Solution (2.24) takes form

$$u(x) = u_0 \mathrm{cn}\left(\sqrt{u_0^2 - 1}x, k\right), \tag{2.25}$$

and for coordinates of the points $\mathbf{p}$ and $\mathbf{q}$ we have

$$\mathbf{p} = (u(-L_0/2),\, u'(-L_0/2)) = (u_s, u_s'); \tag{2.26}$$

$$\mathbf{q} = (u(L_0/2), \quad u'(L_0/2)) \quad = (u_s, -u_s'). \tag{2.27}$$

Now we use the fact that value of H_0 (2.18) remains the same along the trajectory that connects point $\mathbf{p}$ and the point $(u_0, 0)$ of intersection between trajectory and the u axis. Thus one can write the following relationship:

$$H_0 = -u_0^2 + \frac{u_0^4}{2} = (u_s')^2 - u_s^2 + \frac{u_s^4}{2}. \tag{2.28}$$

On the other hand point $\mathbf{p}$ belong to the separatrix of (2.14) and its coordinates satisfy an equality

$$H_* = (u_s')^2 - u_s^2 - \frac{u_s^4}{2} = 0. \tag{2.29}$$

Comparing (2.28) and (2.29) one can conclude

$$u_s^4 = \frac{u_0^4}{2} - u_0^2. \tag{2.30}$$

The next step is to consider equation (2.24) at the point $\mathbf{q}$, we have

$$u_s = u_0 \mathrm{cn}\left(\frac{\sqrt{u_0^2 - 1}L_0}{2}, k\right). \tag{2.31}$$

Put u_s from (2.30) into (2.31), divide both side of the equality by u_0, and introduce a variable change $4v_0^2 = u_0^2 - 1$. Equation (2.31) takes form

$$\left(\frac{1}{2} - \frac{1}{4v_0^2 + 1}\right)^{1/4} = \mathrm{cn}\left(v_0 L_0, k\right), \quad k = \frac{1}{\sqrt{2}}\sqrt{1 + \frac{1}{4v_0^2}}. \tag{2.32}$$

In order to get final the result we need to simplify the expression (2.32). First of all consider k as a function of v_0 and expand it into a series:

$$k(v_0) = \frac{1}{\sqrt{2}} + \frac{1}{8\sqrt{2}}\frac{1}{v_0^2} - \frac{1}{32\sqrt{2}}\frac{1}{v_0^4} + \dots. \tag{2.33}$$

Let $k_0 = 1/\sqrt{2}$ and introduce a remainder $\Delta k = k(v_0) - k_0$. We keep in mind that Δk has a main term of order v_0^{-2} as $v_0 \to \infty$. Denote $w_0 = v_0 L_0$, consider $\mathrm{cn}(w_0, k)$

in the right side of (2.32) as a function of elliptic modulus k and expand it into a series in the vicinity of k_0 up to the second term:

$$\operatorname{cn}(w_0, k_0 + \Delta k) = \operatorname{cn}(w_0, k_0) + f(w_0, k_0)\Delta k + \mathcal{O}(w_0^{-1/4}). \tag{2.34}$$

Here $f(w_0, k_0)$ is the first derivative of elliptic cosine with respect to k at $k = k_0$:

$$f(w_0, k_0) = \frac{\operatorname{sn}(w_0)\operatorname{dn}(w_0)(w_0 - k_0 w_0 + k_0 \operatorname{sn}(w_0)\operatorname{cd}(w_0) - E(\phi(w_0)))}{2(k_0 - 1)k_0}. \tag{2.35}$$

Here $\phi(w, k)$ is the Jacobi amplitude and $E(\phi, k)$ is the incomplete elliptic integral of the second kind. All elliptic functions have the same modulus k_0, we omit this parameter for the sake of brevity. This expression is quite tremendous, nevertheless, what interests us here is the orders of terms with respect to w_0. It has a leading term of order w_0 as $w_0 \to \infty$. That allows us to conclude that the term $f(w_0, k_0)\Delta k$ of (2.34) in its turn has a leading term of order w_0^{-1} (or v_0^{-1}). Rewrite relationship (2.32) in a new form:

$$\left(\frac{1}{2} - \frac{1}{4v_0^2 + 1}\right)^{1/4} = \operatorname{cn}(v_0 L_0, k_0) + \mathcal{O}(v_0^{-1}), \tag{2.36}$$

Using the same approach again we expand the left side of (2.36) into a series:

$$\left(\frac{1}{2} - \frac{1}{4v_0^2 + 1}\right)^{1/4} = \frac{1}{\sqrt[4]{2}} - \frac{1}{2\sqrt[4]{2}}\frac{1}{(4v_0^2 + 1)} + \mathcal{O}(v_0^{-4}). \tag{2.37}$$

Combining (2.37) with (2.36) and comparing the orders of terms we conclude that

$$\operatorname{cn}(v_0 L_0, k_0) = \frac{1}{\sqrt[4]{2}} + \mathcal{O}(v_0^{-1}). \tag{2.38}$$

Let's express $v_0 L_0$ in the equation above

$$v_0 L_0 = \operatorname{cn}^{-1}\left(\frac{1}{\sqrt[4]{2}} + \mathcal{O}(v_0^{-1}), k_0\right) + 2K(k_0)n, \quad n \in \{0\} \cup \mathbb{N}. \tag{2.39}$$

Here $K(k)$ is the complete elliptic integral of the first kind. We left only positive roots since we are interested only in intersections $\mathcal{P}_0(\gamma_1^-) \cap \gamma_2^+$ where u_0 is positive and we can write

$$v_0 = \frac{u_0}{2}\sqrt{1 - \frac{1}{u_0^2}} = \frac{u_0}{2} - \frac{1}{2u_0} + \mathcal{O}(u_0^{-3}). \tag{2.40}$$

We note that by definition of cn^{-1} function

$$\mathrm{cn}^{-1}\left(2^{-1/4}+\mathcal{O}(v_0^{-1})\right)=F\left(\arccos\left(2^{-1/4}+\mathcal{O}(v_0^{-1})\right),k_0\right), \tag{2.41}$$

where $F(\phi,k)$ is incomplete elliptic integral of the first kind. Consider series expansion of arccos up to the main term:

$$\arccos\left(2^{-1/4}+\mathcal{O}(v_0^{-1})\right)=\arccos\left(2^{-1/4}\right)+\mathcal{O}(v_0^{-1}). \tag{2.42}$$

Let's substitute (2.42) into (2.41), use additive property of integral, and apply integral mean value theorem to the second term:

$$\begin{aligned}\mathrm{cn}^{-1}\left(2^{-1/4}+\mathcal{O}(v_0^{-1})\right)&=F\left(\arccos\left(2^{-1/4}\right)+\mathcal{O}(v_0^{-1}),k_0\right)=\\&=F\left(\arccos\left(2^{-1/4}\right),k_0\right)+F\left(\mathcal{O}(v_0^{-1}),k_0\right)=\\&=\mathrm{cn}^{-1}\left(2^{-1/4},k_0\right)+\mathcal{O}(v_0^{-1}).\end{aligned} \tag{2.43}$$

Put (2.43) and (2.40) into (2.39), also note that according to (2.40) we can safely replace $\mathcal{O}(v_0^{-1})$ with $\mathcal{O}(u_0^{-1})$,

$$u_0=\frac{2}{L_0}\left(\mathrm{cn}^{-1}\left(2^{-1/4},k_0\right)+2K(k_0)n\right)+\mathcal{O}(u_0^{-1}). \tag{2.44}$$

Finally let's get rid of u_0 in favor of u_s. For that purpose according to (2.28) we can write $\mathcal{O}\left(H_0^{-1/4}\right)$ instead of $\mathcal{O}(u_0^{-1})$, and it follows from (2.30) that

$$u_s=\frac{1}{\sqrt[4]{2}}u_0+\mathcal{O}(u_0^{-1}). \tag{2.45}$$

Let's introduce the following denotation

$$x_n=\mathrm{cn}^{-1}\left(2^{-1/4},k_0\right)+2K(k_0)n. \tag{2.46}$$

Now combining the expressions above all together and replacing u_s with u_{+n} we get

$$u_{+n}=\frac{2x_{n-1}}{\sqrt[4]{2}L_0}+\mathcal{O}\left(H_0^{-1/4}\right),\quad n\in\mathbb{N}. \tag{2.47}$$

In order to get the final formula of the proposition for $\{u_{+n}\}$ we need to consider points of intersections from the second group $\mathcal{P}_0(\gamma_2^-)\cap\gamma_2^+$. We can easily reduce this task to the previous one. Let there exists a point of intersection $\mathbf{q} \in \gamma_2^+$. Consider point $\mathbf{p} \in \gamma_2^-$, such that $\mathcal{P}_0(\mathbf{p}) = \mathbf{q}$, see Fig. 2.6 (b). We note that there exists a point $\mathbf{p}' \in \gamma_1^-$, and the trajectory (2.24) goes from the point $\mathbf{p}$ to $\mathbf{p}'$ over a half of the period $2K(k)/\sqrt{x_0^2-1}$, and after that cross the u axis at the point u_0. Then we introduce an x variable shift $x \to x - (L_0/2 + K(k)/\sqrt{x_0^2-1})$, so that $u(0) = u_0,\ u_0 > 0$, and $u'(0) = 0$, and can determine $x_0 = u_0,\ x_1 = 0$. Solution (2.24) takes form (2.25) again and for coordinates of the points $\mathbf{p}'$ and $\mathbf{q}$ we have

$$\mathbf{p}' = \left(u\left(-L_0/2 + \tfrac{K(k)}{\sqrt{u_0^2-1}}\right),\ u'\left(-L_0/2 + \tfrac{K(k)}{\sqrt{u_0^2-1}}\right)\right) = (u_s, u_s'); \tag{2.48}$$

$$\mathbf{q} = \left(u\left(L_0/2 - \tfrac{K(k)}{\sqrt{u_0^2-1}}\right),\quad u'\left(L_0/2 - \tfrac{K(k)}{\sqrt{u_0^2-1}}\right)\right) = (u_s, -u_s'). \tag{2.49}$$

Now we can use relationships (2.48), (2.49) instead of (2.26), (2.27), and repeat all the steps above. Difference in x variable shift results in the additional term $K(k)$ in (2.39) and (2.44). Finally we replace $K(k) = K(k_0 + \Delta k) = K(k_0) + \mathcal{O}(H_0^{-2/4})$, and get the following relationship for x_n:

$$x_n = \mathrm{cn}^{-1}\left(2^{-1/4}, k_0\right) + K(k_0)(2n+1). \tag{2.50}$$

Relationship (2.47) remains the same. Combining (2.46) with (2.50) we get the result for separatrix intersections points $\{u_{+n}\} \in \mathcal{P}(\gamma^-) \cap \gamma_2^+$:

$$u_{+n} = \frac{2x_{n-1}}{\sqrt[4]{2}L_0} + \mathcal{O}\left(H_0^{-1/4}\right), \quad n \in \mathbb{N}, \tag{2.51}$$

where x_n satisfies the relationship

$$x_n = \mathrm{cn}^{-1}\left(2^{-1/4}, k_0\right) + K(k_0)n. \tag{2.52}$$

Points $\{u_{-n}\},\ n \in \mathbb{N}$ from the left side of u' axis, $u_{-n} \in \mathcal{P}_0(\gamma^-) \cap \gamma_1^+$, should be treated in a similar way, proposition is proven. □

Propositions 6 says that the far we goes from the $(0,0)$ point on the phase plane, the better the asymptotic relationship (2.22) works. It turns out that formula (2.22) works pretty well even for small number of n. See Figure 2.7 where we compare the predicted coordinates with actual intersections obtained by numerical computation of $\mathcal{P}_0(\gamma^-)$. Another interesting consequence of Proposition 6 is that set $\mathscr{U}_L$ consists of infinitely many connected components. This obviously follows from that fact, that set $\mathscr{U}^-_{L_*}$ contains the entire curve γ^- and map $\mathcal{P}_0$ is continuous, so the image $\mathcal{P}_0(\mathscr{U}^-_{L_*})$ cross $\mathscr{U}^+_L$ infinitely many times.

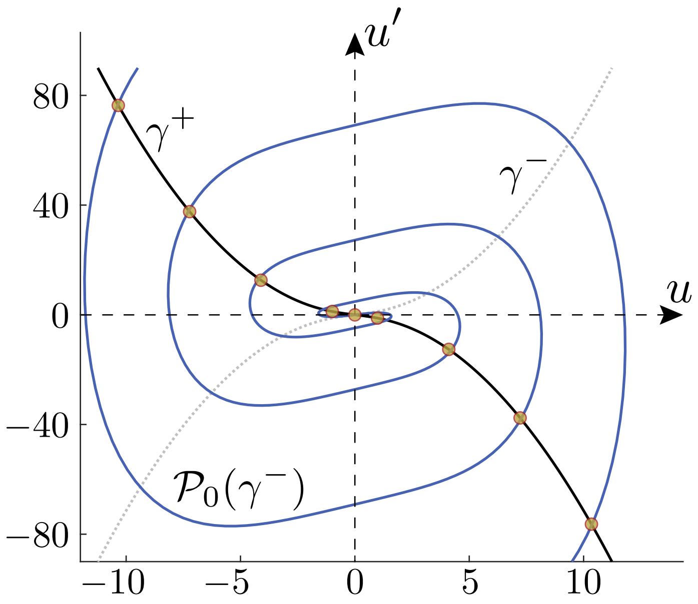

Figure 2.7. Comparison of the relationship (2.22) from Proposition 6 with numerical computations. Curves $\gamma^{\pm}$ are formed by the separatrices of (2.14), $\mathcal{P}_0$-image of γ^- is a solid blue line computed numerically. Predicted points of intersections $u_{\pm n}$ from $\mathcal{P}_0(\gamma^-) \cap \gamma^+$ are marked with yellow dots. One can see that (2.22) predicts intersections quite precisely even for small number of n.

2.3.2. Construction of the Poincaré Map Domains

One of the possible way to construct $\mathscr{U}^{\pm}_L$ sets for different maps associated with stationary states equation (2.1) is to use a numerical procedure called scanning of initial conditions plane (u, u'). That's how it works. At first ranges of scanning $u_{\min} \leq u \leq u_{\max}$, $u'_{\min} \leq u' \leq u'_{\max}$ are selected. Then the target segment of the initial conditions plane is covered by a uniform grid with small steps h and h' for each axis u and u'. Using Runge-Kutta 4th order method we solve differential equation in each node of the result grid. We use an interval $[0; L]$ for $\mathscr{U}^+_L$ where x changes in forward direction from 0 to L, and an interval $[-L; 0]$ in order to get

$\mathscr{U}_L^-$ where x changes in backward direction from 0 to $-L$. If absolute value of a calculated solution does not exceed some huge predefined constant M we suppose that such solution is non-collapsing, and include corresponding node point into $\mathscr{U}_L^\pm$ sets. Then we color non-collapsing nodes on the initial conditions plane to get the final picture of $\mathscr{U}_L^\pm$ sets. In our experiments we used $M = 10^5$ and $M = 10^7$, and got consistent results. Such procedure is pretty straightforward and can be efficiently performed by a computer since it admits natural parallelization. Let's apply this procedure to equation (2.13).

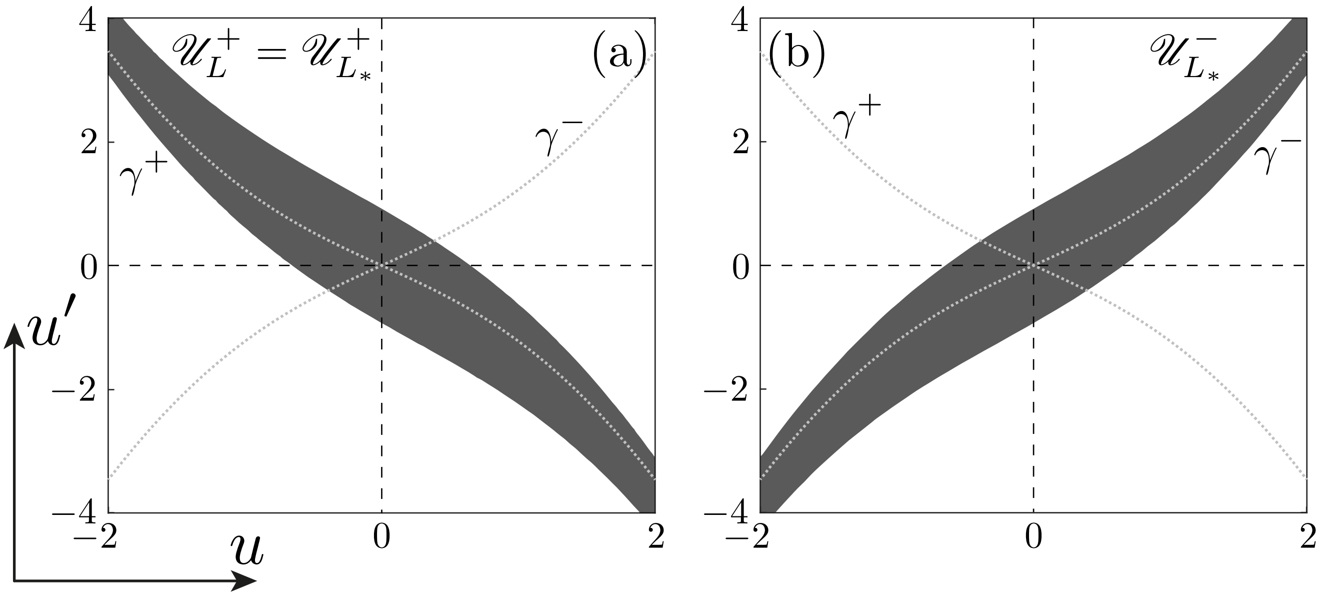

Figure 2.8. Sets $\mathscr{U}_{L_*}^\pm$ for the equation (2.14) for the parameter $L_* = 2$. Panel (a) represents $\mathscr{U}_{L_*}^+$ set, it coincides with the set $\mathscr{U}_L^+$ for equation (2.13), since all solutions of the second equation (2.15) are regular. Panel (b) depicts $\mathscr{U}_{L_*}^-$ set, it's just a reflection of the set $\mathscr{U}_L^+$ from the right panel due to Proposition 4.

On Figure 2.8 (a) Poincaré map domain $\mathscr{U}_L^+ = \mathscr{U}_{L_*}^+$ for the parameters $(L_*, L_0) = (2, 1)$ is depicted. As we mentioned above it contains the curve γ^+ formed by separatrices of (2.14). Figure 2.8 (b) represents a $\mathcal{P}_*$-image of $\mathscr{U}_{L_*}^+$, $\mathcal{P}_*(\mathscr{U}_{L_*}^+) = \mathscr{U}_{L_*}^-$. According to Proposition 4 set $\mathcal{P}_*(\mathscr{U}_{L_*}^-)$ can be obtained by a reflection of the set $\mathscr{U}_{L_*}^+$, with respect to the u' axis. Set $\mathscr{U}_{L_*}^-$ in its turn contains curve γ^-.

Let's continue our scanning in order to get set $\mathscr{U}_L^-$ and then intersect it with $\mathscr{U}_L^+$. On Figure 2.9 (a) set $\mathscr{U}_L^-$ and its intersection with $\mathscr{U}_L^+$ set are depicted for values of parameters $(L_*, L_0) = (2, 1)$. From our numerical procedure we can conclude that intersection $\mathscr{U}_L = \mathscr{U}_L^+ \cap \mathscr{U}_L^-$ form a three-island set in the scanning area $-2 \leq u \leq 2$, $-4 \leq u' \leq 4$, denote them by D_i, $i \in \{-1, 0, +1\}$. Indeed, along with the monotonicity of the connected components borders we also know that two opposite borders of D_i, which entirely belong to the borders of the set $\mathscr{U}_L^+$, consist of points that are mapped to infinity under action of $\mathcal{P}$ (by construction of $\mathscr{U}_L^+$). On other hand borders of $\mathscr{U}_L^-$ contain two other borders of each D_i, and they are mapped to infinity under action of $\mathcal{P}^{-1}$. Thereby the obtained structure satisfy all the conditions of island set from Definition 4. However set $\mathscr{U}_L^-$ entirely contains an image of the curve γ^-. We know that according to Proposition 6 image $\mathcal{P}(\gamma^-)$ has infinitely many intersections with the curve γ^+. That's why outside of the scanning area there exist many other intersections between $\mathscr{U}_L^\pm$ sets and they form infinitely many connected components in the result set $\mathscr{U}_L$. Due to monotonicity of $\mathscr{U}_L^+$ borders and general geometric properties of the spiral $\mathscr{U}_L^-$ we can hypothesize that all other intersections in $\mathscr{U}_L$ set are also islands.

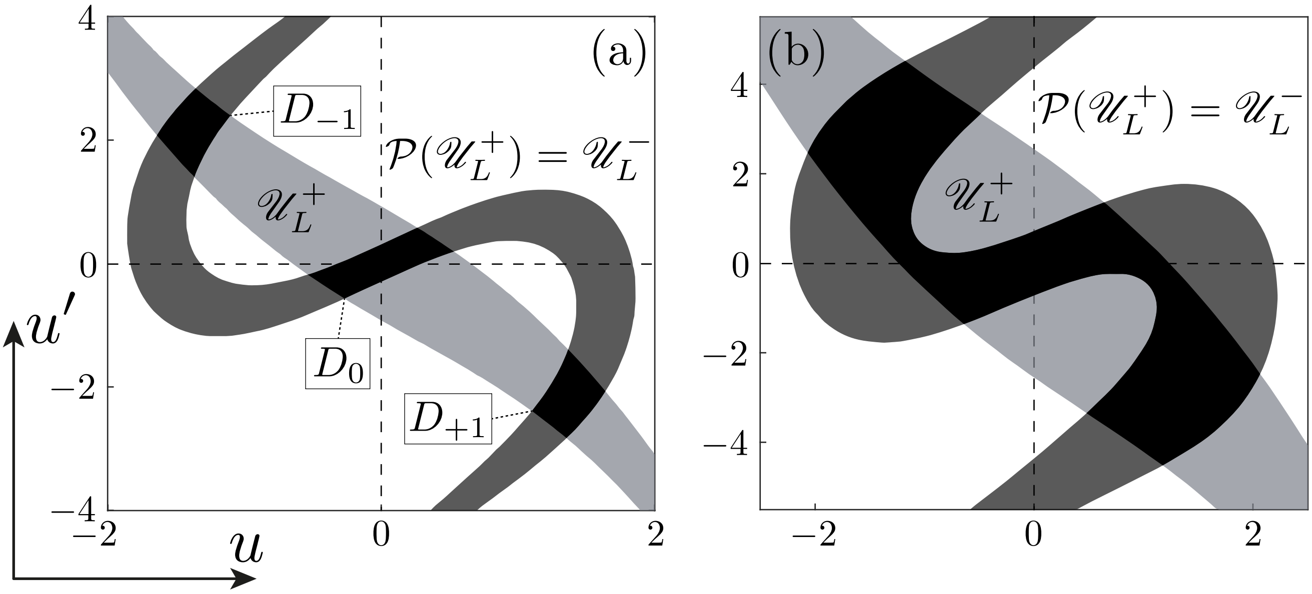

Figure 2.9. Sets $\mathscr{U}_L^+$ (light gray), $\mathscr{U}_L^-$ (dark gray), and their intersection $\mathscr{U}_L$ for two different sets of parameters. Panel (a) depict the case $(L_*, L_0) = (2, 1)$; three central connected components D_i form an island set. Panel (b) correspond to the case $(L_*, L_0) = (1.3, 1)$; geometry of the result sets does not allow to form islands.

Our numerical studies shows that for equation (2.13) three central components of $\mathscr{U}_L$ play a crucial role in an island set formation. For example on Figure 2.1 (b) geometry of the $\mathscr{U}_L^-$ for parameters $(L_*, L_0) = (1.3, 1)$ does not allow to form an island around the center. Establishing a criteria of island set existence is a quite tricky task even for a simple form of stationary states equation with periodic pseudopotential $P(x)$, like (2.13), and such criteria is out of scope for the current work. Our approach here and after is based on scanning of a sufficiently large subset of initial conditions plane around the center $(u, u') = (0, 0)$. If the result subset of $\mathscr{U}_L$ form an island set we just *make a hypothesis* that all other intersections and also islands.

2.3.3. Complete Islands Set

Let $\mathscr{U}_L$ represents an island set. It turns out that for Eq. (2.13) the property of "completeness" for an island set in a sense of Definition 8 naturally arises from its construction. Let's demonstrate it in a non-strict manner. At first, upper boundary of the set $\mathscr{U}_L^+ = \mathscr{U}_{L_*}^+$ consist of such points that the corresponding solution to the Cauchy problem with initial conditions at these points tends to $+\infty$ exactly at the point $x = L_*$. This can be easily followed from the phase portrait for equation (2.14). We can say that such points are mapped to $(+\infty, +\infty)$ under action of $\mathcal{P}_*$, i.e. are mapped to infinity toward the right upper corner on the phase plane. From that perspective lower boundary of the set $\mathscr{U}_L^+$ consists of points that are mapped to $(-\infty, -\infty)$ by $\mathcal{P}_*$, i.e. are mapped to infinity toward the left lower corner on the phase plane.

Let's consider a curve Γ inside one of islands $D_i \in \mathscr{U}_L$ that connects opposite boundaries of the set $\mathscr{U}_L^+$. Denote by Γ_* its $\mathcal{P}_*$-image, $\Gamma_* = \mathcal{P}_*(\Gamma)$. It's clear that Γ_* belongs to $\mathscr{U}_{L_*}^-$, and it's stretched out continuously from $-\infty$ to $+\infty$ by u inside $\mathscr{U}_{L_*}^-$. Now consider the second map $\mathcal{P}_0$ of the decomposition $\mathcal{P} = \mathcal{P}_0\mathcal{P}_*$. We know that this map curls the set $\mathscr{U}_{L_*}^-$ into a spiral (see Fig. 2.9 (a)). This spiral intersects $\mathscr{U}_L^+$ and form islands. So if we consider the $\mathcal{P}_0$-image of Γ_* and take into account that the value of H_0 remains the same for all trajectories of (2.15) associated with $\mathcal{P}_0$ map, we can conclude that $\mathcal{P}_0(\Gamma_*)$ is stretched along the whole set $\mathscr{U}_L^-$ and intersects each of the islands $D_i \in \mathscr{U}_L$ at least once. Such reasoning leads us to the conclusion that all islands in $\mathscr{U}_L$ are forward-reachable. Similar consideration shows that islands from $\mathscr{U}_L$ are also backward-reachable and the constructed island set is complete.

Let's illustrate this idea. For that purpose we construct $\mathcal{P}_*$ and $\mathcal{P}$-images of islands from Figure 2.9 (a). Again we do this numerically with the scanning procedure described above. On Figure 2.10 (a) one can see the $\mathcal{P}_*$-image of islands D_i, $i \in \{-1, 0, +1\}$. As we have expected these images represent infinite curvilinear strips stretched inside the $\mathcal{P}_*$-image of the $\mathscr{U}_L^+$ set. Islands $\mathcal{P}$-images depicted on Figure 2.10 (b). Images $\mathcal{P}(D_i)$ represents infinite curvilinear strips curled up inside the $\mathscr{U}_L^-$ set.

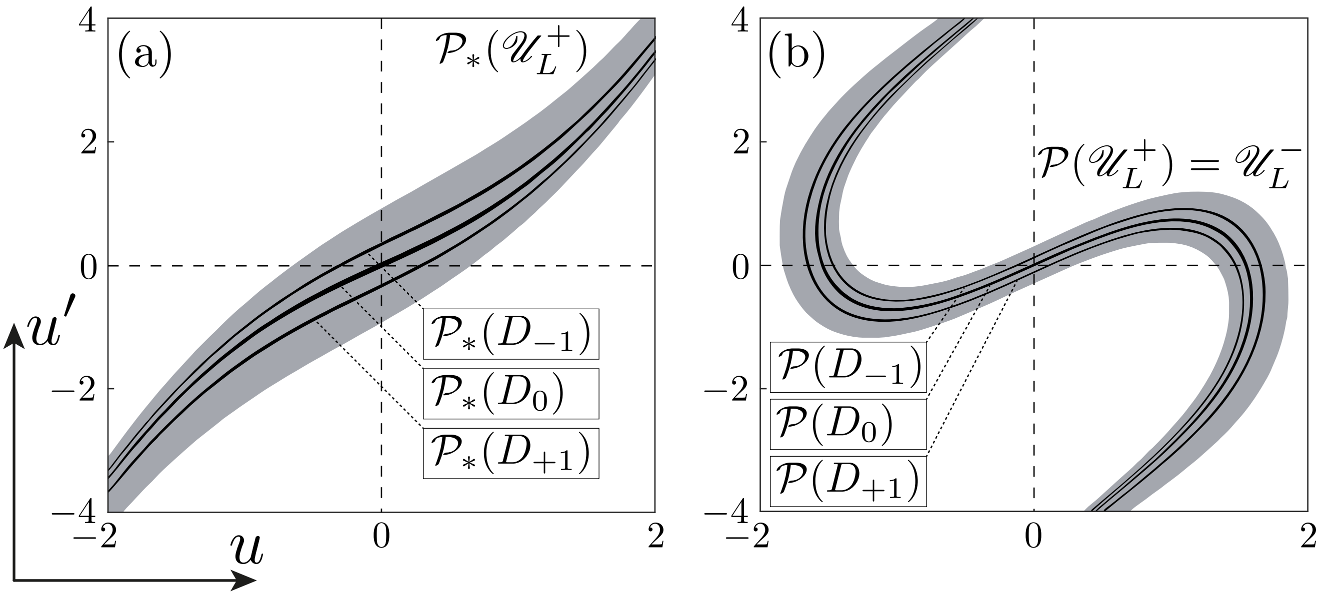

Figure 2.10. $\mathcal{P}_*$ and $\mathcal{P}$-images of islands formed for Eq. (2.13) for parameters $(L_*, L_0) = (2, 1)$. Panel (a) represents their $\mathcal{P}_*$-images. Each image is a curvilinear strip stretched along the whole $\mathcal{P}_*(\mathscr{U}_L^+)$. Panel (b) represents $\mathcal{P}$-images.

Images $\mathcal{P}(D_i)$ remind the behaviour of the separatrices curve image $\mathcal{P}_0(\gamma^-)$. Each of them intersects the $\mathscr{U}_L^+$ set infinitely many times and cross each island from $\mathscr{U}_L$. To illustrate that on Figure 2.11 we combined Figure 2.10 (b) with Figure 2.9 (a). We use the following notation $\mathcal{P}(D_i) \cap D_j = H_{ij}$.

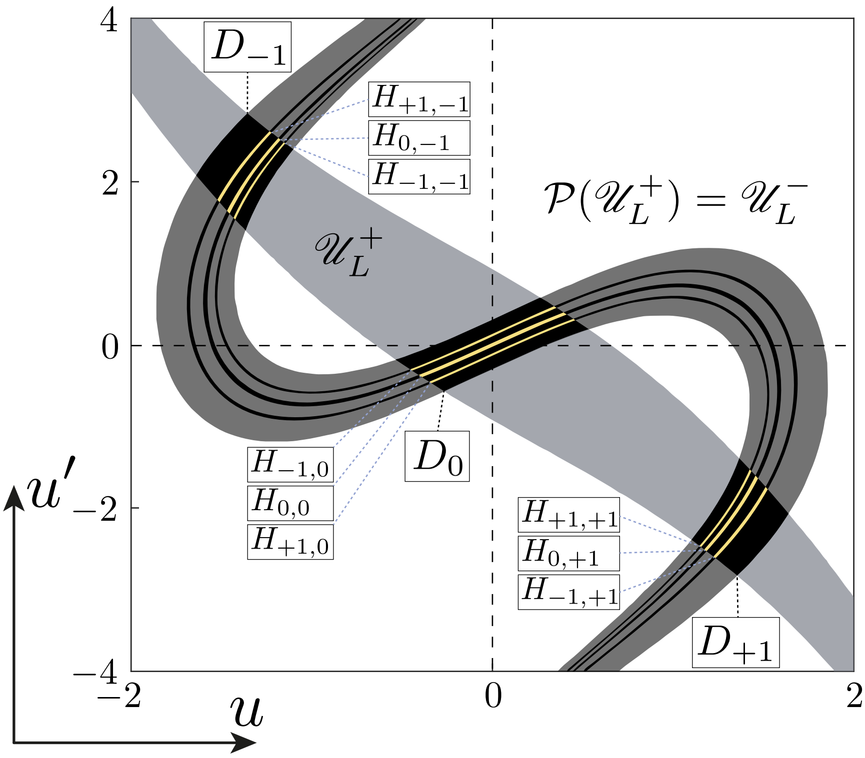

Figure 2.11. Island set $\mathscr{U}_L = \mathscr{U}_L^+ \cap \mathscr{U}_L^-$ and sets $H_{ij} = \mathcal{P}(D_i) \cap D_j$, $i, j \in \{-1, 0, +1\}$ for equation (2.13) with parameters $(L_*, L_0) = (2, 1)$. Islands set $\mathscr{U}_L = \bigcup_{i \in S} D_i$ is forward-reachable, so $\mathcal{P}$-image of each island D_i intersects all other islands D_j, $j \in S$ including D_i itself.

The similar illustration can be provided for $\mathcal{P}^{-1}$ map as well. Island set $\mathscr{U}_L = \bigcup_{i \in S} D_i$ for Eq. (2.13) is backward-reachable. It means that $V_{ij} = \mathcal{P}^{-1}(D_i) \cap D_j \neq \varnothing$ for each $i, j \in S$. On Figure 2.12 sets V_{ij} are depicted for $i, j \in \{-1, 0, +1\}$.

2.4. Symbolic Dynamics: Solutions Coding

In this sections we show how all the structures and properties introduced above can be used together to classify all bounded solutions of equation (2.1). Our classification is closely connected with the structure of the $\mathscr{U}_L$ set. We demonstrate our approach for the previously considered piecewise pseudopotential equation (2.13). Let's introduce two sets.

Definition 12. *Define set $\mathcal{O}$ as a set of all orbits of regular solutions for equation (2.1), i.e. $\{\mathbf{p}_n\} \in \mathcal{O}$, $\mathcal{P}(\mathbf{p}_n) = \mathbf{p}_{n+1}$, where $\mathcal{P}$ is a Poincaré map associated with equation (2.1).*

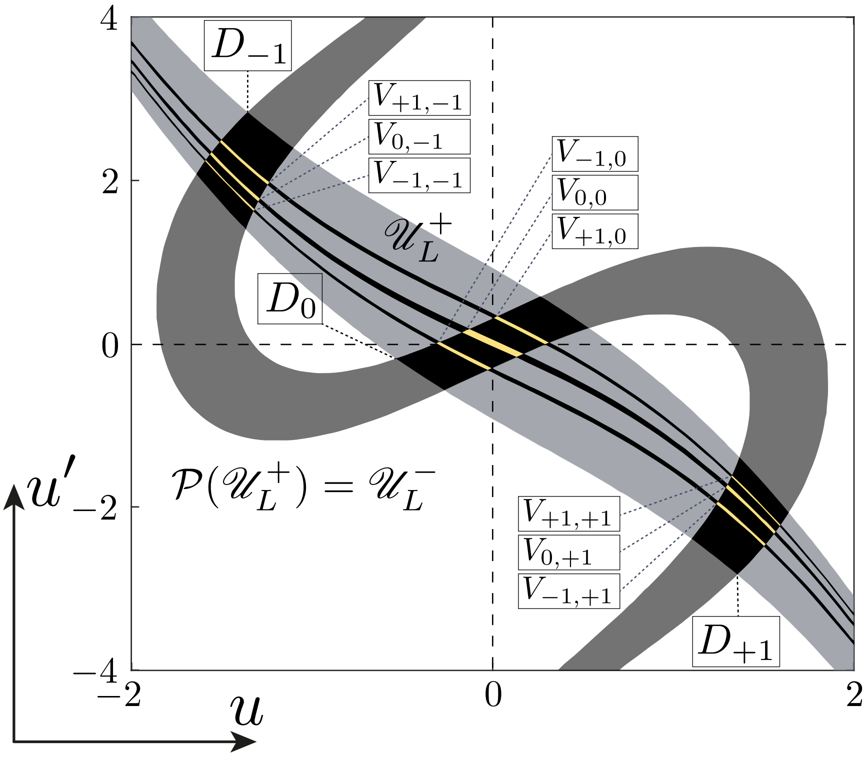

Figure 2.12. Island set $\mathscr{U}_L = \mathscr{U}_L^+ \cap \mathscr{U}_L^-$ and sets $V_{ij} = \mathcal{P}^{-1}(D_i) \cap D_j$, $i, j \in \{-1, 0, +1\}$ for equation (2.13) with parameters $(L_*, L_0) = (2, 1)$. Islands set $\mathscr{U}_L = \bigcup_{i \in S} D_i$ is backward-reachable, so $\mathcal{P}$-pre-image of each island D_i intersects all other islands D_j, $j \in S$ including D_i itself.

One can define a metric $\mathcal{O}$ as follows. Let $v, w \in \mathcal{O}$ are two orbits, $v = \{\mathbf{p}_n\}$, $\mathbf{p}_n = (\phi_n, \phi'_n)$, $w = \{\mathbf{q}_n\}$, $\mathbf{q}_n = (\psi_n, \psi'_n)$, then the distance $d_\mathcal{O}$ between orbits v and w is defined as a Euclidean distance between points $\mathbf{p}_0$ and $\mathbf{q}_0$, i.e.

$$d_\mathcal{O}(v, w) = ||\mathbf{p}_0 - \mathbf{q}_0|| = \sqrt{(\phi_0 - \psi_0)^2 + (\phi'_0 - \psi'_0)^2}. \tag{2.53}$$

This implies that $\mathcal{O}$ can be regarded as a topological space where neighbourhood $U_\varepsilon(u^*)$ of an element $u^* \in \mathcal{O}$ is defined as $U_\varepsilon(u^*) = \{u \mid d_\mathcal{O}(u^*, u) < \varepsilon\}$.

Definition 13. *Define set $\mathcal{S}$ as a set of bi-infinite sequences $\{\dots, i_{-1}, i_0, i_1, \dots\}$ over an alphabet where each symbol i_k, $k = 0, \pm 1, \dots$, corresponds to a connected component $D_k \in \mathscr{U}_L$.*

We also write $\mathcal{S}_N$ if the alphabet has N different symbols, and $\mathcal{S}_\infty$ if the number of symbols is infinite (corresponds to the infinite number of connected components in $\mathscr{U}_L$). Set $\mathcal{S}$ also can be regarded as a topological space where neighbourhood $W_k(\omega^*)$

of an element $\omega^* = \{\dots, i^*_{-1}, i^*_0, i^*_1, \dots\} \in \mathcal{S}$ is defined as $W_k(\omega^*) = \{\omega \mid i^*_s = i_s, |s| < k\}$.

What we are interested in is the connection between sets $\mathcal{O}$ and $\mathcal{S}$. First of all the structure of island set $\mathscr{U}_L$ can be easily used to assign symbolic sequences, also named codes, to the solutions, so the correspondence from $\mathcal{O}$ to $\mathcal{S}$ can be trivially established. Let's demonstrate it with an example. Let one has a regular solution $u(x)$ of equation (2.13). Suppose that this is a localized solution depicted on Figure 2.13 (a). We inspect the values and the derivatives of the solution $u(x)$ in the points corresponding to the Poincaré sections associated with the period L, and then put these points (u, u') onto the structure of the set $\mathscr{U}_L$ from the Panel (b) of Figure 2.13. In the points $x = 0$ value and derivative $\mathbf{p}_0 = (u(0), u'(0))$ matches island D_{-1}. After that in the point $x = L$ our solution $u(x)$ cross the central islands D_0 and matches it again for $x = 2L$. In the point $x = 3L$ our solution came into the right island D_{+1}. That allows us to determine four central symbols of the result code: $\{-1, 0, 0, +1\}$. Moreover since our solution is localized all other points $(u(nL), u'(nL))$ correspond to the central component of $\mathscr{U}_L$ and all the symbols from the left side of "-1" and the right side of "$+1$" are "0". So, finally we obtain the result bi-infinite sequence $\{\dots, 0, -1, 0, 0, +1, 0, \dots\}$ for the localized solution $u(x)$ from Figure 2.13 (a). Obviously points of orbit of our solution cannot lie down outside of $\mathscr{U}_L$ because the solution is regular and has bi-infinite orbit, so at each step we have exactly one symbol and the overall process identifies the result bi-infinite sequence uniquely.

2.4.1. Uniqueness of Solutions Coding

2.5. Summary

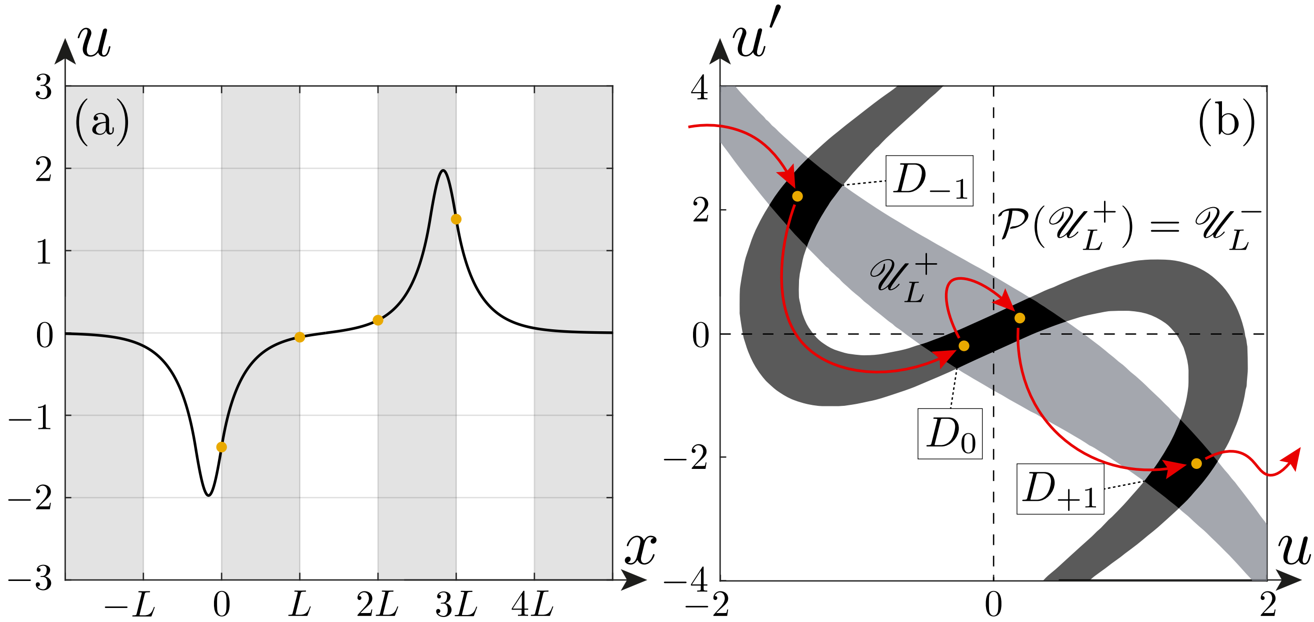

Figure 2.13. Illustration of the coding process. Panel (a) represents a localized solution for the Eq. (2.13) with parameters $(L_*, L_0) = (2, 1)$. This solution has been found numerically using the shooting method. Panel (b) represents a sketch of four points (yellow dots) of the solution orbit over the structure of the $\mathscr{U}_L$ set. These points cross the islands accordingly to the red arrows and determine the symbols of the result solution code: $\{\dots, 0, -1, 0, 0, +1, 0, \dots\}$.

Appendix A

Lemma on Bounded Solutions

Lemma (On bounded solutions)**.** *Let $f(t, z)$ be a function that is continuous with respect to t and continuously differentiable with respect to z. Let $f(t, z)$ is defined for $t \geq t_0$, $|z| < +\infty$, and have the following properties:*

(i) for $|z| < \rho$, $\rho > 0$, the estimate $|f(t, z)| < \eta_\rho(t)|z|$ is valid, where $\eta_\rho(t) \in L_1(t_0; +\infty)$;

(ii) for all z_1, z_2 such that $|z_{1,2}| < \rho$, $\rho > 0$, there exists function $\tilde{\eta}_\rho(t) \in L_1(t_0; +\infty)$, such that $|f(t, z_2) - f(t, z_1)| \leq \tilde{\eta}_\rho(t)|z_2 - z_1|$;

(iii) for $|z| < \rho$, $\rho > 0$, the estimate $|f_z(t, z)| < \theta_\rho(t)|z|$ is valid, where $\theta_\rho \in L_1(t_0, +\infty)$;

(iv) for all z_1, z_2 such that $z_{1,2} < \rho$, $\rho > 0$, there exists function $\tilde{\theta}_\rho \in L_1(t_0; +\infty)$, such that $|f_z(t, z_2) - f_z(t, z_1)| \leq \tilde{\theta}_\rho |z_2 - z_1|$.

Then for the equation

$$z_{tt} - \alpha z_t + f(t, z) = 0, \quad \alpha > 0 \tag{A.1}$$

the following statements are valid:

(A) for each solution $z(t)$ of the equation (A.1) that is bounded when $t \to +\infty$ there exists $C \in \mathbb{R}$ such that $z(t) \to C$ as $t \to +\infty$;

(B) for each $C \in \mathbb{R}$ there exists unique solution $Z(t, C)$ of the equation (A.1), defined on a segment $(t_C; +\infty)$, such that

$$Z(t, C) = C + o(1), \quad t \to +\infty; \tag{A.2}$$

(C) family of solutions $Z(t, C)$ is C^1-smooth with respect to the parameter C.

Proof. Let us prove the statement (A) first. With the method of variation of parameters one can find that a solution of the equation (A.1) satisfies the equality:

$$z(t) = \varkappa_1 + \varkappa_2 e^{\alpha t} + \int_{t_0}^{t} e^{\alpha\eta} \left(\int_{\eta}^{+\infty} e^{-\alpha\xi} f(\xi, z(\xi)) d\xi \right) d\eta. \tag{A.3}$$

It follows from the condition (i) that if $z(t)$ is bounded while $t \to +\infty$ then the integral

$$\int_{t_0}^{+\infty} e^{\alpha\eta} \left(\int_{\eta}^{+\infty} e^{-\alpha\xi} f(\xi, z(\xi)) d\xi \right) d\eta \tag{A.4}$$

converges. Furthermore for all bounded solutions $\varkappa_2 = 0$, hence $z(t)$ tends to some constant for $t \to +\infty$. That proves the point (A).

Move on to the point (B). We make a variable change $u(t) = z(t) - C$, where C is an arbitrary number. Rewrite the equation (A.1) in the form of a system of equations

$$y_t = Ay + F(t, y), \tag{A.5}$$

where

$$y = \begin{pmatrix} u \\ v \end{pmatrix}, \quad A = \begin{pmatrix} 0 & 1 \\ 0 & \alpha \end{pmatrix}, \quad F(t, y) = \begin{pmatrix} 0 \\ f(t, u + C) \end{pmatrix}.$$

Now we apply Theorem 9.1 from [10, Chapter XII] to the system (A.5). It states that the system (A.5) *has a solution which tends to zero at infinity* <u>if</u> the following conditions are satisfied:

(1) function $F(t, y)$ is continuous and $||F(t, y)|| \leq \lambda(t)$ for $t \in [t_0; +\infty)$, $||y|| \leq \rho$, where $\lambda(t) \in L_1(t_0; +\infty)$;

(2) for all $g(t) = col(g_1(t), g_2(t))$, $g(t) \in L_1(t_0; +\infty)$ there exists a solution $y(t) \in L_0^\infty(t_0; +\infty)$ of the inhomogeneous system

$$y_t = Ay + g(t); \tag{A.6}$$

(hereinafter by the norm $|| \cdot ||$ we mean the Euclidean norm in $\mathbb{R}$).

At first, by the condition (i) if $|u| \leq \rho$ and $t > t_0$ relation $||f(t,u,C)|| \leq \rho\eta_\rho(t)$ takes place, moreover $\eta_\rho \in L_1(t_0;+\infty)$, hence the condition (1) of the above-mentioned theorem is satisfied. At second, general solution of the inhomogeneous system of equations (A.6) can be written as:

$$u(t) = C_2 + \int\limits_{t_0}^{t} \left(g_1(\eta) + e^{\alpha\eta} \left(C_1 - \int\limits_{+\infty}^{\eta} e^{-\alpha\xi} g_2(\xi) d\xi \right) \right) d\eta; \tag{A.7}$$

$$v(t) = u_t(t) - g_1(t). \tag{A.8}$$

Since $g_{1,2}(t) \in L_1(t_0;+\infty)$ one can choose appropriate parameters C_1, C_2 in order to get a solution which tends to zero while $t \to +\infty$, so the condition (2) of the theorem is also met. Thereby both of the conditions for the applied theorem take place for the system (A.5). That implies existence of a solution $z(t)$ of (A.1) that approaches a given constant C while $t \to +\infty$ for all C.

Now we prove the uniqueness of such solution. Suppose that for the same C there exist two solutions $u_{1,2}(t)$ for equation

$$u_{tt} - \alpha u_t + f(t, u + C) = 0. \tag{A.9}$$

Consider their difference $\Delta(t) = u_2(t) - u_1(t)$, it satisfies the equation

$$\Delta_{tt} - \alpha\Delta_t + R(t)\Delta = 0, \tag{A.10}$$

and a boundary condition $\Delta \to 0$ as $t \to +\infty$ takes place. Here

$$R(t) \equiv \frac{f(t, u_2(t) + C) - f(t, u_1(t) + C}{u_2(t) - u_1(t)}. \tag{A.11}$$

By the condition (ii) we can apply Theorem 11 from [11, Chapter 3]. It states that there exists a homeomorphism between the bounded solutions of the equation (A.10) and solutions of equation

$$\Delta_{tt} - \alpha\Delta_t = 0, \tag{A.12}$$

moreover (see a note to that theorem in [11]) this homeomorphism is a linear map. It means that only a zero solution of (A.10) satisfies the zero asymptotic at infinity, i.e. $u_2(t) \equiv u_1(t)$. Thus we have proven the existence of the solutions family $Z(t, C)$ parametrised by $C \in \mathbb{R}$, statement (B) is proven.

To prove the statement (C) one can note that the derivative

$$\frac{\partial Z}{\partial C}(t, C) \equiv \Theta(t, C) \tag{A.13}$$

satisfies the equation (A.9) after differentiation with respect to C, moreover $\Theta(t, C) \to 0$ as $t \to +\infty$. We have

$$\Theta_{tt} - \alpha\Theta_t + f_z(t, u + C)\Theta + f_z(t, u + C) = 0. \tag{A.14}$$

Here we can use Theorem 11 from [11, Chapter 3] again, and using the condition (iii) we can conclude that there exists a solution of this equation $\Theta(t, C)$ such that $\Theta(t, C) \to 0$ as $t \to +\infty$, and function $\Theta(t, C)$ is continuous with respect to the parameter C. That proves the overall lemma. $\square$

Appendix B

Solutions of Duffing equations

Appendix C

Strips Mapping Theorems

Theorem 1 (On h-strips mapping)**.** *Let Poincaré map* $\mathcal{P}$ *and its inverse* $\mathcal{P}^{-1}$ *are defined on a complete (see Definition 8) island set* $\bigcup_{i\in S} D_i$*, where* S *is a finite or countable set of indices. Let for all* $i, j \in S$ *set* $V_{ji} = \mathcal{P}^{-1}D_j \cap D_i$ *is non-empty,* $\mathcal{P}$ *is defined on a closure* $\overline{V_{ji}}$*, and one of the following two conditions is met:*

(1) borders $\alpha_i^{\pm}$ *of an island* D_i *are increasing curves,* $\forall \mathbf{p} \in \overline{V_{ji}}$ *signs of values* $\{a_{mn}\}$ *in the matrix of the linear operator* $D\mathcal{P}_{\mathbf{p}} = (a_{mn})$ *have exactly one of the following configurations*:*

$$(a)\ \left(\begin{smallmatrix} + & + \\ + & + \end{smallmatrix}\right), \quad (b)\ \left(\begin{smallmatrix} - & - \\ - & - \end{smallmatrix}\right), \quad (c)\ \left(\begin{smallmatrix} + & + \\ - & - \end{smallmatrix}\right), \quad (d)\ \left(\begin{smallmatrix} - & - \\ + & + \end{smallmatrix}\right);$$

and at the same time borders $\alpha_j^{\pm}$ *of* D_j *are increasing curves for cases (a), (b), and decreasing curves for (c), (d);*

(2) borders $\alpha_i^{\pm}$ *of an island* D_i *are decreasing curves,* $\forall \mathbf{p} \in \overline{V_{ji}}$ *signs of values* $\{a_{mn}\}$ *in the matrix of the linear operator* $D\mathcal{P}_{\mathbf{p}} = (a_{mn})$ *have exactly one of the following configurations:*

$$(a)\ \left(\begin{smallmatrix} + & - \\ - & + \end{smallmatrix}\right), \quad (b)\ \left(\begin{smallmatrix} - & + \\ + & - \end{smallmatrix}\right), \quad (c)\ \left(\begin{smallmatrix} + & - \\ + & - \end{smallmatrix}\right), \quad (d)\ \left(\begin{smallmatrix} - & + \\ - & + \end{smallmatrix}\right);$$

and at the same time borders $\alpha_j^{\pm}$ *of* D_j *are decreasing curves for cases (a), (b), and increasing for (c), (d);*

and moreover $\exists \mu > 1$ *such that* $\forall p \in \overline{V_{ji}}$, $|a_{11}| \geq \mu$*, then for any* h*-strip* $H \in D_i$*,* $\mathcal{P}(H) \cap D_j = \widetilde{H}_j$ *is also an* h*-strip, and* $d_{\mathrm{h}}(\widetilde{H}_j) \leq (1/\mu) d_{\mathrm{h}}(H)$ *(here* $d_{\mathrm{h}}(\cdot)$ *is an* h*-strip thickness in a sence of Definition 9).*

*By "+" and "−" sign we mean strict inequalities $a_{mn} > 0$, $a_{mn} < 0$ to be held.

Proof. Let's fix indices i, j and prove the theorem for a pair of islands D_i, D_j. Mostly we consider the case (1a). Other cases The rest of the cases must be treated in a completely analogous way. Denote by $\mathbf{e}_1$, $\mathbf{e}_2$ basis vectors

$$\mathbf{e}_1 = \begin{pmatrix} 1 \\ 0 \end{pmatrix}; \quad \mathbf{e}_2 = \begin{pmatrix} 0 \\ 1 \end{pmatrix}. \tag{C.1}$$

Define the following set of *cones*:

$$\begin{aligned}
\mathbb{R}^2_{++} &= \{\mathbf{v} \,|\, \mathbf{v} = x\mathbf{e}_1 + y\mathbf{e}_2,\ x > 0, y > 0\}; \\
\overline{\mathbb{R}}^2_{++} &= \{\mathbf{v} \,|\, \mathbf{v} = x\mathbf{e}_1 + y\mathbf{e}_2,\ x \geq 0, y \geq 0\}; \\
\mathbb{R}^2_{+-} &= \{\mathbf{v} \,|\, \mathbf{v} = x\mathbf{e}_1 + y\mathbf{e}_2,\ x > 0, y < 0\}; \\
\overline{\mathbb{R}}^2_{+-} &= \{\mathbf{v} \,|\, \mathbf{v} = x\mathbf{e}_1 + y\mathbf{e}_2,\ x \geq 0, y \leq 0\}; \\
\mathbb{R}^2_{-+} &= \{\mathbf{v} \,|\, \mathbf{v} = x\mathbf{e}_1 + y\mathbf{e}_2,\ x < 0, y > 0\}; \\
\overline{\mathbb{R}}^2_{-+} &= \{\mathbf{v} \,|\, \mathbf{v} = x\mathbf{e}_1 + y\mathbf{e}_2,\ x \leq 0, y \geq 0\}; \\
\mathbb{R}^2_{--} &= \{\mathbf{v} \,|\, \mathbf{v} = x\mathbf{e}_1 + y\mathbf{e}_2,\ x < 0, y < 0\}; \\
\overline{\mathbb{R}}^2_{--} &= \{\mathbf{v} \,|\, \mathbf{v} = x\mathbf{e}_1 + y\mathbf{e}_2,\ x \leq 0, y \leq 0\}.
\end{aligned}$$

As a first step in the proof, we show that values signs in the matrix of linear operator $D\mathcal{P}_{\mathbf{p}} = (a_{mn})$ uniquely determine the structure of cones mapping in each point $\mathbf{p}$ of the set $\overline{V_{ji}}$. For the case (a) we have:

$$\forall \mathbf{v} = \begin{pmatrix} x \\ y \end{pmatrix} \in \overline{\mathbb{R}}^2_{++},\ D\mathcal{P}_{\mathbf{p}}(\mathbf{v}) = \begin{pmatrix} a_{11} & a_{12} \\ a_{21} & a_{22} \end{pmatrix} \begin{pmatrix} x \\ y \end{pmatrix} = \begin{pmatrix} \widetilde{x} > 0 \\ \widetilde{y} > 0 \end{pmatrix} \in \mathbb{R}^2_{++}.$$

It is easy to check that the complete scheme of the cones mapping for the case (1) of the theorem looks as follows:

$$\begin{aligned}
&\text{(a)}\quad D\mathcal{P}_{\mathbf{p}}(\overline{\mathbb{R}}^2_{++}) \in \mathbb{R}^2_{++}, \quad D\mathcal{P}_{\mathbf{p}}(\overline{\mathbb{R}}^2_{--}) \in \mathbb{R}^2_{--}; \\
&\text{(b)}\quad D\mathcal{P}_{\mathbf{p}}(\overline{\mathbb{R}}^2_{++}) \in \mathbb{R}^2_{--}, \quad D\mathcal{P}_{\mathbf{p}}(\overline{\mathbb{R}}^2_{--}) \in \mathbb{R}^2_{++}; \\
&\text{(c)}\quad D\mathcal{P}_{\mathbf{p}}(\overline{\mathbb{R}}^2_{++}) \in \mathbb{R}^2_{+-}, \quad D\mathcal{P}_{\mathbf{p}}(\overline{\mathbb{R}}^2_{--}) \in \mathbb{R}^2_{-+}; \\
&\text{(d)}\quad D\mathcal{P}_{\mathbf{p}}(\overline{\mathbb{R}}^2_{++}) \in \mathbb{R}^2_{-+}, \quad D\mathcal{P}_{\mathbf{p}}(\overline{\mathbb{R}}^2_{--}) \in \mathbb{R}^2_{+-}.
\end{aligned}$$

Complete scheme for the case (2) have the following form correspondingly:

$$
\begin{aligned}
&\text{(a)}\quad D\mathcal{P}_{\mathbf{p}}(\overline{\mathbb{R}}^2_{-+}) \in \mathbb{R}^2_{-+}, \quad D\mathcal{P}_{\mathbf{p}}(\overline{\mathbb{R}}^2_{+-}) \in \mathbb{R}^2_{+-};\\
&\text{(b)}\quad D\mathcal{P}_{\mathbf{p}}(\overline{\mathbb{R}}^2_{-+}) \in \mathbb{R}^2_{+-}, \quad D\mathcal{P}_{\mathbf{p}}(\overline{\mathbb{R}}^2_{+-}) \in \mathbb{R}^2_{-+};\\
&\text{(c)}\quad D\mathcal{P}_{\mathbf{p}}(\overline{\mathbb{R}}^2_{-+}) \in \mathbb{R}^2_{--}, \quad D\mathcal{P}_{\mathbf{p}}(\overline{\mathbb{R}}^2_{+-}) \in \mathbb{R}^2_{++};\\
&\text{(d)}\quad D\mathcal{P}_{\mathbf{p}}(\overline{\mathbb{R}}^2_{-+}) \in \mathbb{R}^2_{++}, \quad D\mathcal{P}_{\mathbf{p}}(\overline{\mathbb{R}}^2_{+-}) \in \mathbb{R}^2_{--}.
\end{aligned}
$$

As a <u>second</u> step we show that such cones mapping preserve in some way Lipschitz constraints and monotonicity properties for curves from $\overline{V_{ji}}$ under the $\mathcal{P}$ mapping. Show that for the case (1a). For that first of all we note that from compactness of $\overline{V_{ji}}$ the existence of the following supremum follows:

$$
\widetilde{\gamma}_{ji} = \sup \frac{y}{x}, \quad \begin{pmatrix} x \\ y \end{pmatrix} = D\mathcal{P}_{\mathbf{p}}(\mathbf{v}), \ \mathbf{p} \in \overline{V_{ji}}, \ \mathbf{v} \in \overline{\mathbb{R}}^2_{++}.
$$

Further, let there be two tow different points $\mathbf{p}_1\,\mathbf{p}_2 \in \overline{V_{ji}}$, $\mathbf{p}_1 = (\psi_1, \psi_1')$, $\mathbf{p}_2 = (\psi_2, \psi_2')$, and besides $\psi_2 \geq \psi_1$, $\psi_2' \geq \psi_2$. Let points $\mathbf{q}_1$, $\mathbf{q}_2$ be the $\mathcal{P}$-images of the points $\mathbf{p}_1$, $\mathbf{p}_2$ correspondingly, $\mathcal{P}(\mathbf{p}_1) = \mathbf{q}_1 = (\phi_1, \phi_1')$, $\mathcal{P}(\mathbf{p}_2) = \mathbf{q}_2 = (\phi_2, \phi_2')$. Let $D\mathcal{P}_{\mathbf{p}_1}$ is a linearization of $\mathcal{P}$ at the point $\mathbf{p}_1$. Then the following expansion is valid:

$$
\mathbf{q}_2 = \mathcal{P}(\mathbf{p}_2) = \mathbf{q}_1 + D\mathcal{P}_{\mathbf{p}_1}(\mathbf{p}_2 - \mathbf{p}_1) + r(||\mathbf{p}_2 - \mathbf{p}_1||), \tag{C.2}
$$

where $r(||\mathbf{p}_2 - \mathbf{p}_1||)/||\mathbf{p}_2 - \mathbf{p}_1|| \to 0$ as $||\mathbf{p}_2 - \mathbf{p}_1|| \to 0$ (here $|||\cdot||$ is a Euclidean norm). Vector $\mathbf{p}_\Delta = \mathbf{p}_2 - \mathbf{p}_1 \in \overline{\mathbb{R}}^2_{++}$ which means that for its mapping by linearized operator we have $D\mathcal{P}_{\mathbf{p}_1}(\mathbf{p}_\Delta) = \mathbf{q}_\Delta \in \mathbb{R}^2_{++}$, and

$$
\mathbf{q}_2 - \mathbf{q}_1 = \mathbf{q}_\Delta + r(||\mathbf{p}_2 - \mathbf{p}_1||). \tag{C.3}
$$

Expression above means that for "close enough" points $\mathbf{p}_1$, $\mathbf{p}_2$ their images satisfy the relationship $\mathbf{q}_2 - \mathbf{q}_1 \in \mathbb{R}^2_{++}$, i.e. $\phi_2 > \phi_1$, $\phi_2' > \phi_1'$. Moreover one can choose a value $\gamma_{ji} > \widetilde{\gamma_{ji}}$ such that the following inequality is held:

$$
0 < \phi_2' - \phi_1' < \gamma_{ji}(\phi_2 - \phi_1). \tag{C.4}
$$

This ordering is transitive, i.e. from the relation (C.4) and the second analogous relation for "close enough" point $\mathbf{p}_2$, $\mathbf{p}_3$,

$$0 < \phi_3' - \phi_2' < \gamma_{ji}(\phi_3 - \phi_2), \tag{C.5}$$

follow the analogous relation for the points $\mathbf{p}_1$, $\mathbf{p}_3$ as well. That allows to spread the relation (C.4) over all points $\mathbf{p}_1,\ \mathbf{p}_2 \in \overline{V_{ji}}$ that satisfies the conditions $\psi_2 \geq \psi_1$, $\psi_2' \geq \psi_1'$. Other cases (1b)-(1d), (2a)-(2d) can be considered in a similar way.

Thus for the case (1) for all points $\mathbf{p}_1,\ \mathbf{p}_2 \in \overline{V_{ji}}$, which coordinates satisfy the relations $\psi_2 \geq \psi_1$, $\psi_2' \geq \psi_1'$, coordinates of their $\mathcal{P}$-images $\mathbf{q}_1 = (\phi_1, \phi_1')$, $\mathbf{q}_2 = (\phi_2, \phi_2')$ depending on sings of values in matrix of $D\mathcal{P}_{\mathbf{p}}$, $\mathbf{p} \in \overline{V_{ji}}$, met exactly one of the following inequalities ($\exists \gamma_{ji}$):

$$\text{(a)} \quad 0 < \phi_2' - \phi_1' < \gamma_{ji}(\phi_2 - \phi_1); \tag{C.6a}$$

$$\text{(b)} \quad 0 < \phi_1' - \phi_2' < \gamma_{ji}(\phi_1 - \phi_2); \tag{C.6b}$$

$$\text{(c)} \quad 0 < \phi_1' - \phi_2' < \gamma_{ji}(\phi_2 - \phi_1); \tag{C.6c}$$

$$\text{(d)} \quad 0 < \phi_2' - \phi_1' < \gamma_{ji}(\phi_1 - \phi_2). \tag{C.6d}$$

For the case (2) in its turn we have that for all points $\mathbf{p}_1,\ \mathbf{p}_2 \in \overline{V_{ji}}$, which coordinates satisfy the relations $\psi_2 \leq \psi_1$, $\psi_2' \geq \psi_1'$, exactly one of the following inequalities is met:

$$\text{(a)} \quad 0 < \phi_2' - \phi_1' < \gamma_{ji}(\phi_1 - \phi_2); \tag{C.7a}$$

$$\text{(b)} \quad 0 < \phi_1' - \phi_2' < \gamma_{ji}(\phi_2 - \phi_1); \tag{C.7b}$$

$$\text{(c)} \quad 0 < \phi_1' - \phi_2' < \gamma_{ji}(\phi_1 - \phi_2); \tag{C.7c}$$

$$\text{(d)} \quad 0 < \phi_2' - \phi_1' < \gamma_{ji}(\phi_2 - \phi_1). \tag{C.7d}$$

A a <u>third</u> step we demonstrate how these inequalities above allow to conclude that for any h-strip $H \in D_i$ its image $\mathcal{P}H \cap D_j = \widetilde{H}_j$ is also an h-strip. Let an h-strip $H \in D_i$ is placed between two monotonic h-curves $\widetilde{\alpha}_i^{\pm}$. Endpoints of the $\widetilde{\alpha}_i^{\pm}$ belong to the boundaries $\beta_i^{\pm}$ of island D_i, so the H is a curvilinear quadrangle bounded by curves $\widetilde{\alpha}_i^{\pm}$ and segments of curves $\beta_i^{\pm}$. For the case (1a) of the theorem curves $\widetilde{\alpha}_i^{\pm}$ are increasing. Let's consider an image of the curve $\widetilde{\alpha}_i^{+}$. According to the definition of a complete island set $\mathcal{P}(\widetilde{\alpha}_i^{+})$ cross each of the boundaries $\beta_j^{\pm}$ of island D_j at least once. At the same time $\mathcal{P}(\widetilde{\alpha}_i^{+})$ cannot cross boundaries $\alpha_j^{\pm}$ because they consist of points which tends to infinity under action of $\mathcal{P}^{-1}$.

Let $\mathcal{P}(\widetilde{\alpha}_i^{+})$ cross one of the boundaries $\beta_j^{\pm}$ of the island D_j twice. Denote those intersection points by $\mathbf{q}_1 = \mathcal{P}(\mathbf{p}_1)$, $\mathbf{q}_2 = \mathcal{P}(\mathbf{p}_2)$. For the case (1a) boundaries $\alpha_j^{\pm}$ are increasing curves, and $\beta_j^{\pm}$ are decreasing, hence the points $\mathbf{q}_1$, $\mathbf{q}_2$ belong to a decreasing curve. From the other side points $\mathbf{p}_1,\ \mathbf{p}_2 \in \overline{V_{ji}}$ belong to increasing curve $\widetilde{\alpha}_i^{+}$, and hence for their $\mathcal{P}$-image coordinates $\mathbf{q}_1 = (\phi_1, \phi_1')$, $\mathbf{q}_2 = (\phi_2, \phi_2')$ inequality (C.6a) must be held. This inequality means that points $\mathbf{q}_1$, $\mathbf{q}_2$ cannot belong to a decreasing curve, and $\mathcal{P}(\widetilde{\alpha}_i^{+})$ cross each boundary $\beta_j^{\pm}$ only once. Similar statement is valid also for the $\mathcal{P}(\widetilde{\alpha}_i^{-})$. Thereby $\mathcal{P}(\widetilde{\alpha}_i^{\pm}) \cap D_j$ are monotonic curves. Their type of monotonicity coincide with the monotonicity type of corresponding boundaries of the island D_j, moreover these curves bound the set $\mathcal{P}H \cap D_j$, hence $\mathcal{P}H \cap D_j = \widetilde{H}_j$ is an h-strip. Other cases can be considered in a similar way using the corresponding inequalities (C.6b) – (C.6d), (C.7a) – (C.7d).

Finally, in a <u>fourth</u> step of this proof we show that under the introduced constrain on $|a_{11}|$ value of linearized operator, for all h-strip $H \in D_i$, $\rho(\widetilde{H}_j) \leq \mu\rho(H)$, so that thickness of an h-strip $\mathcal{P}$-image within island D_j is less than thickness of an original h-strip inside island D_i. To prove that first assume that h-strips H and $\widetilde{H}_j$ are well-measured in a sense on Definition 10. Let the thickness of the h-strip $\widetilde{H}_j$ can be measured along the vertical curve connecting points $\mathbf{q}_1 = (\phi_1, \phi_1')$, $\mathbf{q}_2 = (\phi_2, \phi_2')$, $\phi_1' < \phi_2'$. Consider a parametrization of that curve $\mathbf{q}(t) = (0, \phi'(t))$, where

$$\phi'(t) = t\phi_2' + (1-t)\phi_1', \quad 0 \leq t \leq 1. \tag{C.8}$$

Strip $\widetilde{H}_j$ is well-measurable, so the curve $\mathbf{q}(t)$ entirely belongs to $\widetilde{H}_j$. Since $\widetilde{H}_j = \mathcal{P}H \cap D_j$ there exists a pre-image $\mathbf{p}(t) = \mathcal{P}^{-1}(\mathbf{q}(t)) = (\psi(t), \psi'(t))$, $\mathbf{p}(t) \subset H$ and $\mathbf{q}(t) = \mathcal{P}(\mathbf{p}(t))$. For the case (1a) let's demonstrate that $\mathbf{p}(t)$ is a decreasing curve connecting point from the opposite boundaries $\widetilde{\alpha}_i^{\pm}$ of the strip H inside D_i. Remark, here by "decreasing" we mean that the curve is a graph of decreasing function in (u, u') coordinates, not as a function of t. The curve $\mathbf{q}(t)$ belongs to some set which is a $\mathcal{P}$-image of a part of the set $\overline{V_{ji}}$. The signs of values in the matrix of $D\mathcal{P}_{\mathbf{p}}$, $\mathbf{p} \in \overline{V_{ji}}$ have the form $\left(\begin{smallmatrix} + & + \\ + & + \end{smallmatrix}\right)$, so the signs of values for the linearized inverse map $D\mathcal{P}_{\mathbf{q}}^{-1}$ have a configuration $\left(\begin{smallmatrix} + & - \\ - & + \end{smallmatrix}\right)$ on the curve $\mathbf{q}(t)$. This allows to conclude the corresponding cones mapping:

$$D\mathcal{P}_{\mathbf{q}(t)}^{-1}(\overline{\mathbb{R}}_{-+}^2) \in \mathbb{R}_{-+}^2, \quad D\mathcal{P}_{\mathbf{q}(t)}^{-1}(\overline{\mathbb{R}}_{+-}^2) \in \mathbb{R}_{+-}^2. \tag{C.9}$$

Therefore the corresponding monotonicity property (C.7a) takes place. It immediately follows from (C.7a) that the vertical curve $\mathbf{q}(t)$ is mapped to the decreasing curve $\mathbf{p}(t)$ (decreasing in (u, u') coordinates). Moreover the inequality $\phi_1' < \phi_2'$ provides that $\psi'(t) > 0$.

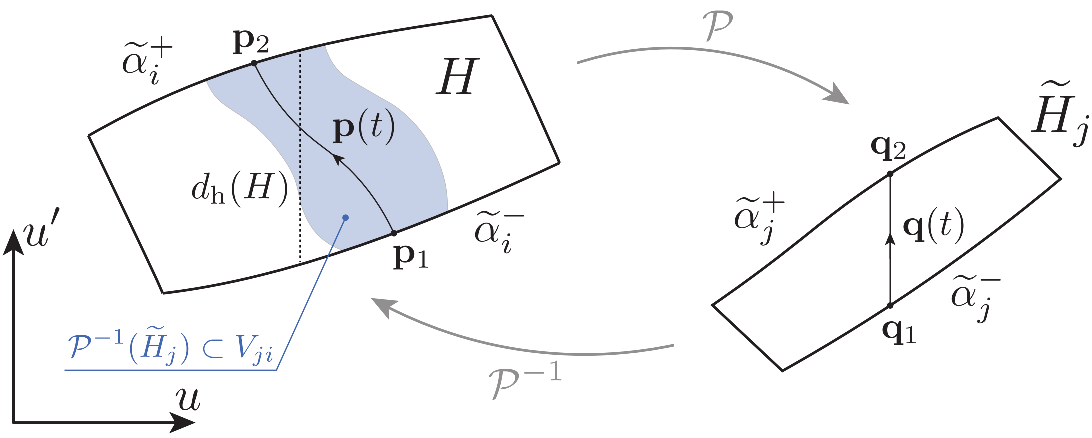

Figure C.1. Illustration for the proof of the h-strips thickness decrease for the case when both h-strips H and $\widetilde{H}_j$ and well-measurable. Thickness of H is measured along the vertical dotted line, thickness of $\widetilde{H}_j$ is measured along the vertical line $\mathbf{q}(t)$. Arrows indicate curves traverse directions while t changes from 0 to 1. Pre-image of $\widetilde{H}_j$ strip is colored with gray.

Consider tangent vectors to $\mathbf{p}(t)$ and $\mathbf{q}(t)$ (upper dot means the derivative with respect to t):

$$\dot{\mathbf{p}}(t) = (\dot{\psi}(t), \dot{\psi}'(t)); \tag{C.10}$$

$$\dot{\mathbf{q}}(t) = (0, \dot{\phi}'(t)). \tag{C.11}$$

In each point t they are connected by the $D\mathcal{P}_{\mathbf{p}(t)}$ operator

$$\dot{\mathbf{q}}(t) = D\mathcal{P}_{\mathbf{p}(t)}(\dot{\mathbf{p}}(t)). \tag{C.12}$$

Rewrite this relation in a matrix form:

$$\begin{pmatrix} a_{11}(t) & a_{12}(t) \\ a_{21}(t) & a_{22}(t) \end{pmatrix} \begin{pmatrix} \dot{\psi}(t) \\ \dot{\psi}'(t) \end{pmatrix} = \begin{pmatrix} 0 \\ \dot{\phi}'(t) \end{pmatrix}. \tag{C.13}$$

We take into account that matrix (a_{mn}) is a linearization of Poincaré map to conclude that its determinant $a_{11}(t)a_{22}(t)-a_{12}(t)a_{21}(t) = 1$ in each point t. From the relations above and the theorem condition on values of $a_{11}(t)$ follows

$$\dot{\phi}'(t) = \frac{1}{a_{11}(t)}\dot{\psi}'(t) \leq \frac{1}{\mu}\dot{\psi}'(t). \tag{C.14}$$

Integration of (C.14) with limits $0 \leq t \leq 1$ gives:

$$d_{\mathrm{h}}(\widetilde{H}_j) = \phi_2' - \phi_1' = \int_0^1 \dot{\phi}'(t)dt \leq \frac{1}{\mu}\int_0^1 \dot{\psi}'(t)dt = \frac{1}{\mu}(\psi_2' - \psi_1'). \tag{C.15}$$

Curve $\mathbf{p}(t)$ is decreasing and boundaries of H are increasing curves, so it follows from general geometric considerations that $\psi_2' - \psi_1' \leq d_{\mathrm{h}}(H)$, i.e. $d_{\mathrm{h}}(\widetilde{H}_j) \leq (1/\mu)d_{\mathrm{h}}(H)$. That gives the final statement of the theorem for well-measurable strips.

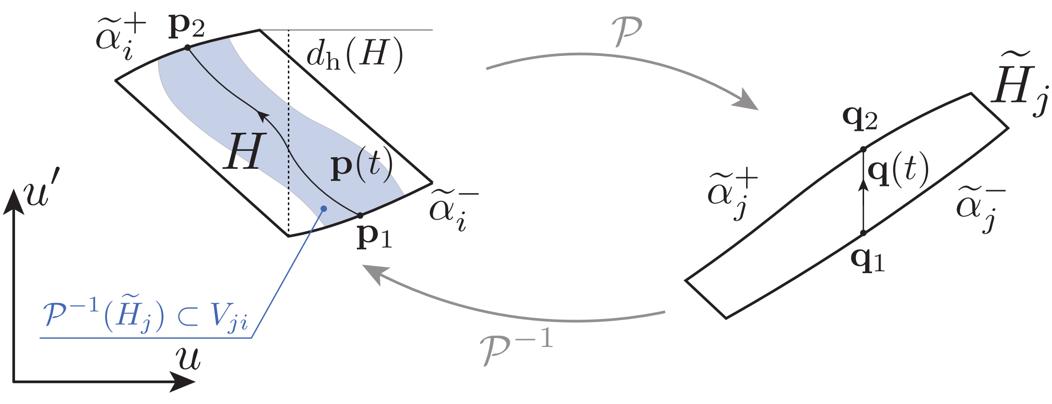

Figure C.2. Illustration for the proof of the h-strips thickness decrease for the case when strip H is not well-measurable. Its thickness is measured along the vertical dotted line. One endpoint of that line does not belong to the strip boundary $\widetilde{\alpha}_i^+$. Pre-image of $\widetilde{H}_j$ strip is colored with gray.

The proof above can be easily generalized to the cases when h-strips H and $\widetilde{H}_j$ are not well-measurable. If strip H is not well-measurable, the inequality $\psi_2' - \psi_1' \leq$

$d_{\mathrm{h}}(H)$ in (C.15) takes place anyway. This fact is illustrated on Figure C.2. Vertical distance between points $\mathbf{p}_1$, $\mathbf{p}_2$ turns out to be certainly less than the width of H strip.

In the case when h-strip $\widetilde{H}_j$ is not well-measurable, one should choose corner points $\mathbf{q}_1$, $\mathbf{q}_2$ in a such way that the vertical distance between them equals the thickness of $\widetilde{H}_j$, and then connect $\mathbf{q}_1$, $\mathbf{q}_2$ with a monotonic decreasing curve $\mathbf{q}(t)$, see Fig. C.3. This is always possible due to the geometric properties of not well-measurable h-strip. According to the choice of points $\mathbf{q}_1$, $\mathbf{q}_2$, $d_{\mathrm{h}}(\widetilde{H}_j) = \phi_2 - \phi_1$, and all the steps above remain valid since the corresponding cones mapping with all the consequences can be also applied for the decreasing curves $\mathbf{p}(t)$ and $\mathbf{q}(t)$.

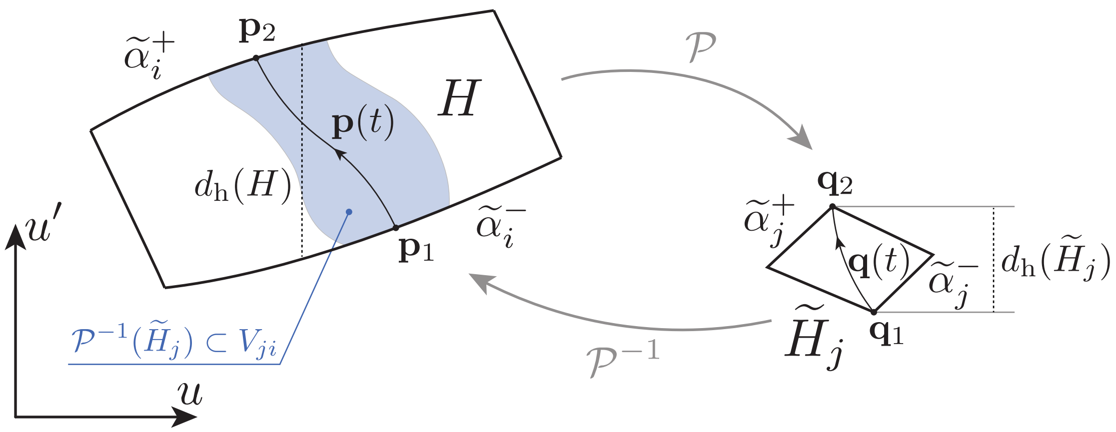

Figure C.3. Illustration for the proof of the h-strips thickness decrease for the case when strip $\widetilde{H}_j$ is not well-measurable. Thickness of H and $\widetilde{H}_j$ are measured along the dotted lines. Pre-image of $\widetilde{H}_j$ strip is colored with gray.

If both h-strips H and $\widetilde{H}_j$ are not well-measurable then two above mentioned technics should be combined together. During the consideration of all other cases of the theorem only type of curves monotonicity is changed, but the overall approach remains the same and can be applied with just minor adjustments. Theorem is proven. $\square$

Theorem 2 (On v-strips mapping)**.** *Let Poincaré map $\mathcal{P}$ and its inverse $\mathcal{P}^{-1}$ are defined on a complete (see Definition 8) island set $\bigcup_{i\in S} D_i$, where S is a finite or countable set of indices. Let for all $i, j \in S$ set $H_{ij} = \mathcal{P}D_i \cap D_j$ is non-empty, $\mathcal{P}^{-1}$ is defined on a closure $\overline{H_{ij}}$, and one of the following two conditions is met:*

(1) borders $\beta_j^\pm$ of an island D_j are increasing curves, $\forall \mathbf{q} \in \overline{H_{ij}}$ signs of values $\{b_{mn}\}$ in the matrix of the linear operator $D\mathcal{P}_{\mathbf{q}}^{-1} = (b_{mn})$ have exactly one of the following configurations:

$$\text{(a)}\ \left(\begin{smallmatrix} + & + \\ + & + \end{smallmatrix}\right), \quad \text{(b)}\ \left(\begin{smallmatrix} - & - \\ - & - \end{smallmatrix}\right), \quad \text{(c)}\ \left(\begin{smallmatrix} + & + \\ - & - \end{smallmatrix}\right), \quad \text{(d)}\ \left(\begin{smallmatrix} - & - \\ + & + \end{smallmatrix}\right);$$

and at the same time borders $\beta_i^\pm$ of D_i are increasing curves for cases (a), (b), and decreasing curves for (c), (d);

(2) borders $\beta_j^\pm$ of an island D_j are decreasing curves, $\forall \mathbf{q} \in \overline{H_{ij}}$ signs of values $\{b_{mn}\}$ in the matrix of the linear operator $D\mathcal{P}_{\mathbf{q}}^{-1} = (b_{mn})$ have exactly one of the following configurations:

$$\text{(a)}\ \left(\begin{smallmatrix} + & - \\ - & + \end{smallmatrix}\right), \quad \text{(b)}\ \left(\begin{smallmatrix} - & + \\ + & - \end{smallmatrix}\right), \quad \text{(c)}\ \left(\begin{smallmatrix} + & - \\ + & - \end{smallmatrix}\right), \quad \text{(d)}\ \left(\begin{smallmatrix} - & + \\ - & + \end{smallmatrix}\right);$$

and at the same time borders $\beta_i^\pm$ of D_i are decreasing curves for cases (a), (b), and increasing for (c), (d);

and moreover $\exists \nu > 1$ such that $\forall q \in \overline{H_{ij}}$, $|b_{22}| \geq \nu$, then for any v*-strip $V \in D_j$, $\mathcal{P}^{-1}(V) \cap D_i = \widetilde{V}_i$ is also a* v*-strip, and $d_{\mathrm{v}}(\widetilde{V}_i) \leq (1/\nu) d_{\mathrm{v}}(V)$ (here $d_{\mathrm{v}}(\cdot)$ is an* v*-strip thickness in a sence of Definition 11).*

Proof. Completely analogous to the proof of the h-strips mapping theorem. $\square$

Bibliography

1. Extreme Tunability of Interactions in a ^{7}Li Bose-Einstein Condensate / S. E. Pollack [et al.] // Phys. Rev. Lett. — 2009. — Mar. — Vol. 102, issue 9. — P. 090402.

2. Feshbach resonances in ultracold gases / C. Chin [et al.] // Rev. Mod. Phys. — 2010. — Apr. — Vol. 82, issue 2. — P. 1225–1286.

3. Combination of a magnetic Feshbach resonance and an optical bound-to-bound transition / D. M. Bauer [et al.] // Phys. Rev. A. — 2009. — June. — Vol. 79, issue 6. — P. 062713.

4. *Hukriede J.*, *Runde D.*, *Kip D.* Fabrication and application of holographic Bragg gratings in lithium niobate channel waveguides. — 01/2003.

5. *Pachpatte B. G.* Inequalities for Differential and Integral Equations. Vol. 197. — Mathematics in Science, Engineering, 1998.

6. *Alfimov G. L.*, *Zezyulin D. A.* Nonlinear modes for the Gross–Pitaevskii equation with periodic potential // Nonlinearity. — 2007. — No. 20. — P. 2075–2092.

7. *Alfimov G. L.*, *Lebedev M. E.* On Regular and Singular Solutions for Equation $u_{xx}+Q(x)u+P(x)u^3$ // Ufa Mathematical Journal. — 2015. — Vol. 7, no. 2. — P. 3–16.

8. *Alfimov G. L.*, *Avramenko A. I.* Coding of nonlinear states for the Gross–Pitaevskii equation with periodic potential // Physica D: Nonlinear Phenomena. — 2013. — Vol. 254. — P. 29–45. — ISSN 0167-2789.

9. *Guckenheimer J.*, *Holmes P.* Nonlinear Oscillations, Dynamical Systems, and Bifurcations of Vector Fields. Vol. 42. — Springer-Verlag New York, 1983. — (Applied Mathematical Sciences).

10. *Hartman P.* Ordinary Differential Equations. — New York: John Wiley, Sons, 1964.

11. *Coppel W. A.* Stability and Asymptotic Behaviour of Differential Equations. — Boston: Heath, Co., 1965.